# High spatial resolution external beams


Lorenzo Giuntini

*Department of Physics,*
*University of Firenze*
*and*
*Istituto Nazionale di Fisica Nucleare,*
*sezione di Firenze,*
*Italy*



**VI Scuola Nazionale "Rivelatori ed Elettronica per Fisica delle Alte Energie, Astrofisica, Applicazioni Spaziali e Fisica Medica"**
**RADFAC 2015 thematic day**
**23-27 Marzo 2015**
**INFN-LNL**

# *Summary*

*introduction - extracted beams: why?*

1. *external beams:*
   - *ion beam induced damage*
   - *beam exit windows*
2. *external microbeam set-ups*
3. *examples of interest in CH field*

*conclusions*

# *Extracted beam*

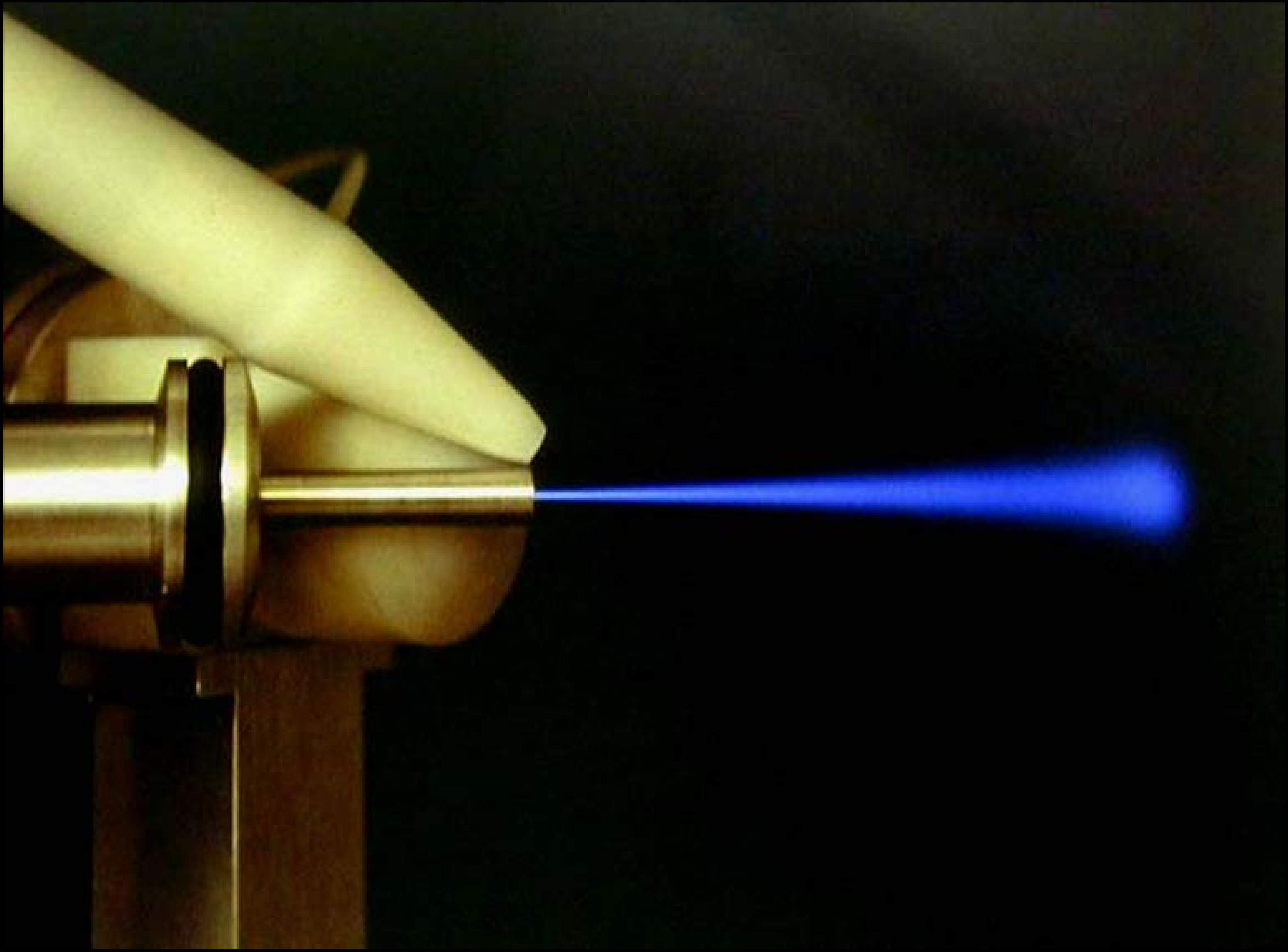

# *External beams: why?*

Advantages:

•no limitations to the dimensions of the objects to analyze

•ease of handling, moving and monitoring the target

•no time-consuming pump-down and vent of the vacuum chamber

•no need for sampling

•effective target heat dissipation

•no charging effects $\Leftrightarrow$ no coating

# *Beam extraction into atmosphere*

Beam extraction into the atmosphere requires some cautions not to degrade beam quality.

Angular and energy straggling induced by the window and the external path in the atmosphere worsen beam quality:

- increase beam angular divergence
- increase beam dimensions
- broaden energy distribution of transmitted ions [$\sigma_E \propto (\rho t)^{0.5}$]

*i.e. the shorter the thickness of the external path* (window + atmosphere), *the better the external beam*

# Polymeric (kapton) 8 μm thick windows

ELSEVIER Nuclear Instruments and Methods in Physics Research B 210 (2003) 75–78

www.elsevier.com/locate/nimb

## In situ monitoring of polyimide windows for external ion microbeams

A. Kinomura *, Y. Mokuno, A. Chayahara, N. Tsubouchi, Y. Horino

*National Institute of Advanced Industrial Science and Technology, 1-8-31 Midorigaoka, Ikeda, Osaka 563-8577, Japan*

**Abstract**

Damage of polyimide windows for external ion microbeams was monitored by analyzing backscattering protons from the window. A 1.5 MeV proton microbeam focused to approximately $50 \times 50$ μm$^2$ was transmitted through the polyimide window from vacuum to oxygen atmosphere. The changes in backscattering spectra of the window were monitored as a function of irradiation dose up to $2 \times 10^{18}$ $H^+/cm^2$. For comparison, the polyimide window was irradiated in vacuum in the same way as the oxygen case. The backscattering spectra drastically changed in the case of oxygen. We observed that the carbon spectrum width, corresponding to the thickness of the window, substantially decreased with increasing the irradiation dose. The in situ monitoring of backscattering protons demonstrated the ability to detect the damage of the window and to predict the rupture of the window.

# 8 μm kapton windows

The spot sizes for the irradiation were about 50 × 50 μm². The proton beam was not scanned during the irradiation. The beam current for the irradiation was adjusted to 1 nA. A Si surface-barrier detector (SSD) was located at a scattering angle of 150° as shown in Fig. 1.



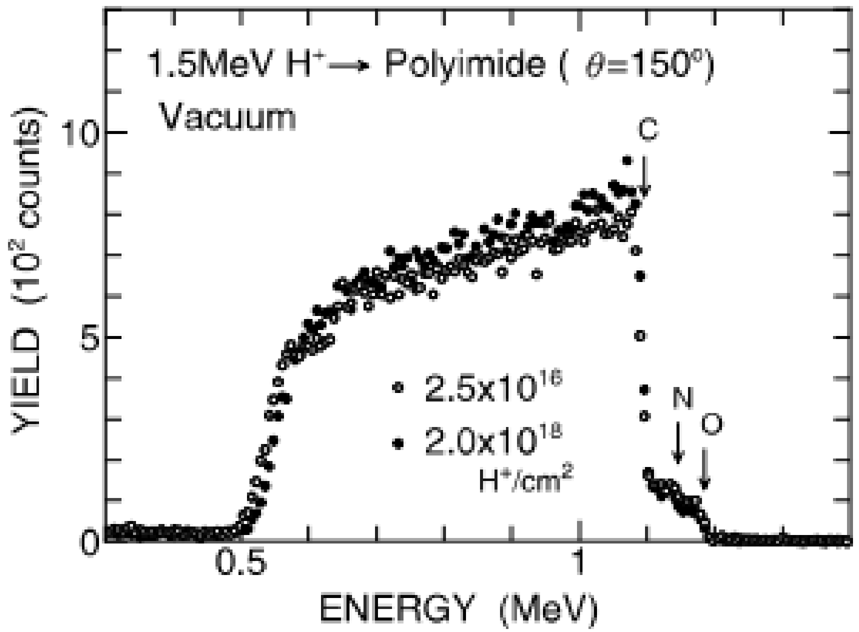


Fig. 2. Backscattering spectra of the polyimide windows irradiated in vacuum. The 1.5 MeV proton microbeam was transmitted from the vacuum side to the vacuum side.

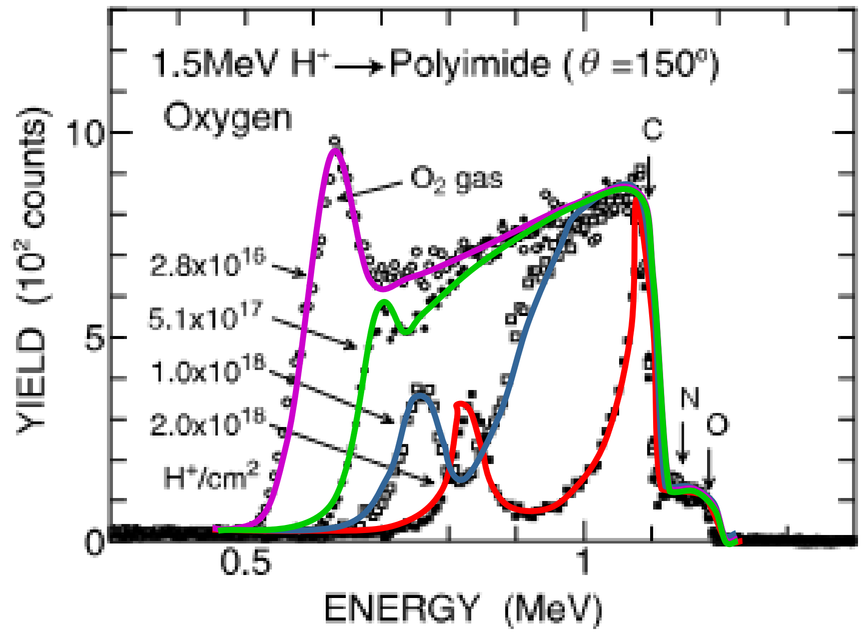


Fig. 3. Backscattering spectra of the polyimide windows irradiated with oxygen atmosphere. The 1.5 MeV proton microbeam was transmitted from the vacuum side to the oxygen side.

# 8 μm kapton windows

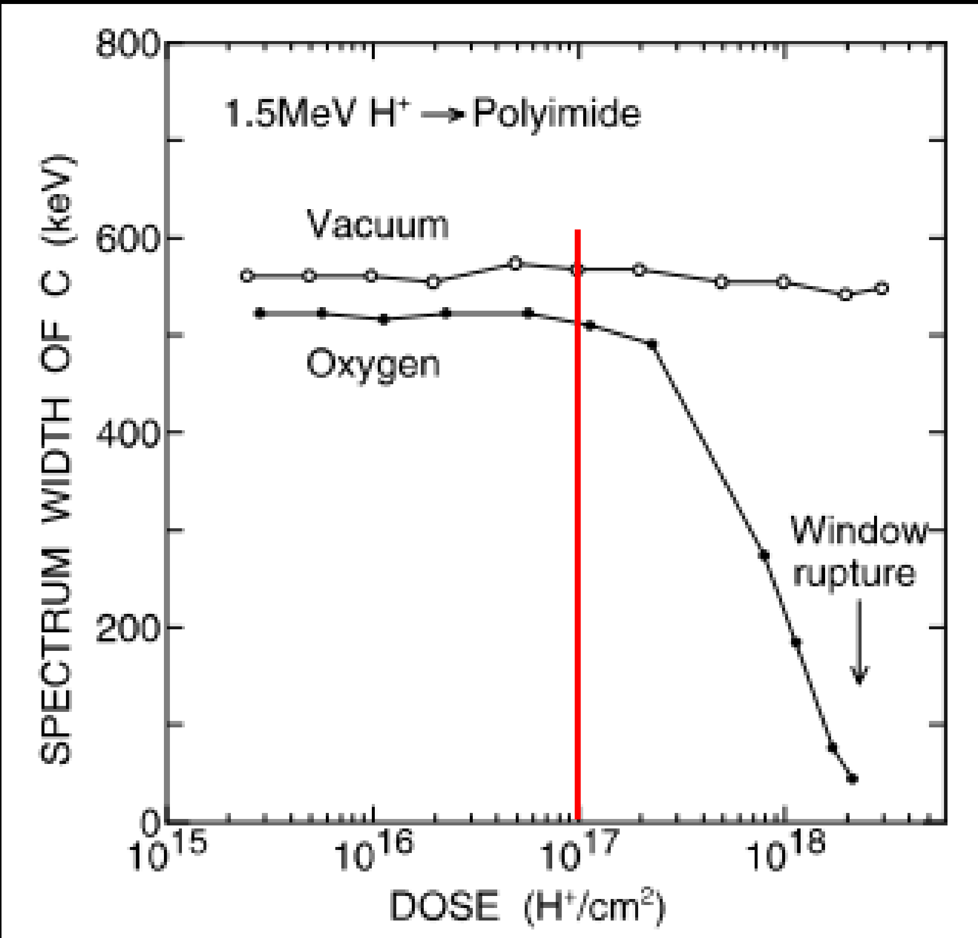


Fig. 4. Spectrum width of carbon as a function of proton dose for the vacuum and the oxygen irradiations. For the irradiation with oxygen atmosphere, a rupture of the polyimide window occurred after the irradiation of $2 \times 10^{18}$ $H^+/cm^2$ as indicated with an arrow. For the irradiation in vacuum, the polyimide window was almost stable in terms of the backscattering spectra.

- let's assume $\phi = 10^{17}$ $H^+ cm^{-2}$ as the fluency security threshold
- incoming beam diameter: 1 μm
- security threshold for 1μm$^2$ beam: $10^9$ $H^+$
- Let's assume a beam current; I = 1.6 nA = 1.6 $10^{-9}$A
- number of ion per second hitting the target: 1.6 $10^{-9}$A/1.6 $10^{-19}$ $H^+s^{-1}$ = $10^{10}$ $H^+s^{-1}$
- window usage time $t_{st}$=100 ms

# Breaking of an 8 μm kapton window

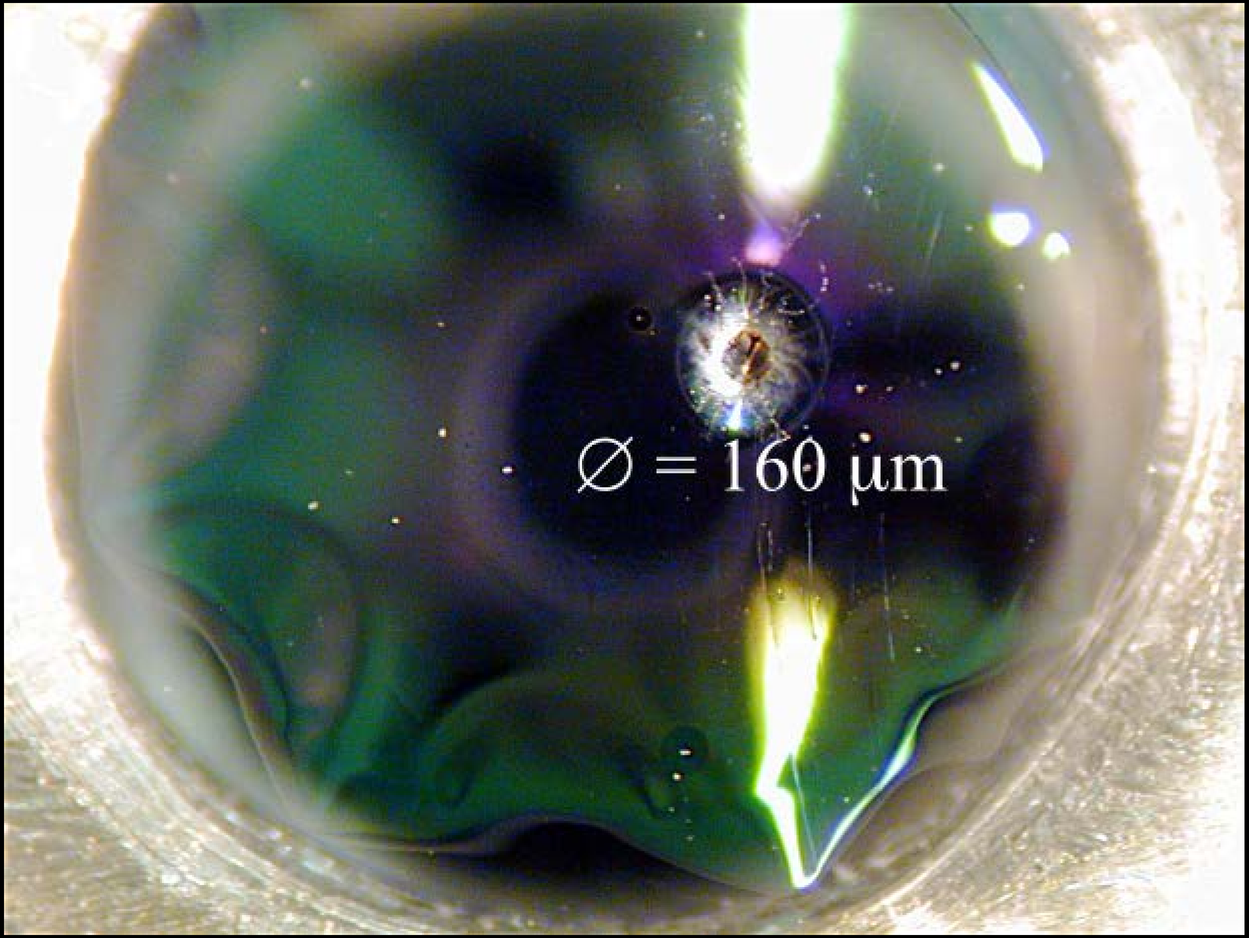

# Non-polymeric windows: *the pioneer study*

ELSEVIER

Nuclear Instruments and Methods in Physics Research Section B: Beam Interactions with Materials and Atoms

Volume 54, Issues 1–3, 2 March 1991, Pages 47–51

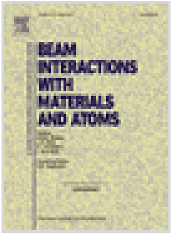


## Thin $Si_3N_4$ windows for energy loss STIM in air

H.W. Lefevre, R.M.S. Schofield

D.R. Ciarlo

### Abstract

The use of thin (102 nm) windows of $Si_3N_4$ to transmit an electronically rastered microbeam of MeV protons into ambient air with small scattering is reported. The windows were made by anisotropic etching of Si, exposing about 1 $mm^2$ of silicon nitride film integrally attached to a silicon supporting frame. Stress measurements on films of several thicknesses yielded a value of Young's modulus of 350 GPa. Energy loss scanning transmission ion micrographs of several small living animals are presented. Focused beams of 100 pA have been passed through the films without failure.

# Non-polymeric windows: a survey

ELSEVIER Nuclear Instruments and Methods in Physics Research B 136–138 (1998) 339–343

## An external milli-beam for archaeometric applications on the AGLAE IBA facility of the Louvre museum

T. Calligaro *, J.-C. Dran, H. Hamon, B. Moignard, J. Salomon

*Laboratoire de Recherche des Musées de France, CNRS UMR171, Palais du Louvre, 75 041 Paris Cedex 01, France*

**Abstract**

External beam lines have been built on numerous IBA facilities for the analysis of works of art to avoid sampling and vacuum potentially detrimental to the integrity of such precious objects. On the other hand, growing interest lies on microprobe systems which provide a high lateral resolution but which usually work under vacuum. Until recently, the AGLAE facility was equipped with separate external beam and microprobe lines. The need of a better spatial resolution in the external beam mode has led us to combine them into a single system which exhibits numerous advantages and allows the analysis of small heterogeneities like inclusions in gemstones or tiny components of composite samples. The triplet of quadrupole lenses bought from Oxford is used to focus the beam. By using a 0.75 µm thick Al foil as the exit window, blowing a helium flow around the beam spot and reducing the window-sample distance below 3 mm, a beam size of about 30 µm can be reached.

# Non-polymeric windows

Table 1
Different exit windows used on the AGLAE external beam line and transmission properties for 3-MeV protons

| Material | Thickness (μm) | Energy loss (keV) | Energy straggling (keV) | Angular divergence (deg) | Minimum spot size achieved (μm) |
|---|---|---|---|---|---|
| Al | 0.75 | 17 | 2.0 | 0.2 | 30 |
| Al | 10 | 233 | 15.9 | 0.8 | 150 |
| Zr | 2 | 73 | 7.3 | 0.85 | 200 |
| Kapton | 8 | 129 | 9.0 | 0.35 | 500 |

Energy loss and straggling as well as angular divergence are based on TRIM calculations which provide the energy and angular distributions of transmitted ions; TRIM data have been subsequently processed with the STATISTICA program. The angular divergence is taken as the standard deviation of the projected angular distribution.

Microbeam setup

For mm-sized beams, the exit window has an area of about 4 mm$^2$ and is made of either a 10 μm Al foil in PIXE mode or of a 2-μm-thick Zr foil in RBS, NRA or PIGE ones. The smaller beam spot of about 20–30 μm (see below) has been obtained with a 0.75 μm thick Al foil supported by a 150 μm thick sapphire wafer with a 100 μm diameter hole.

*100 nm $Si_3N_4$ definitely better than 750 nm Al foil*

*100 nm $Si_3 N_4$*

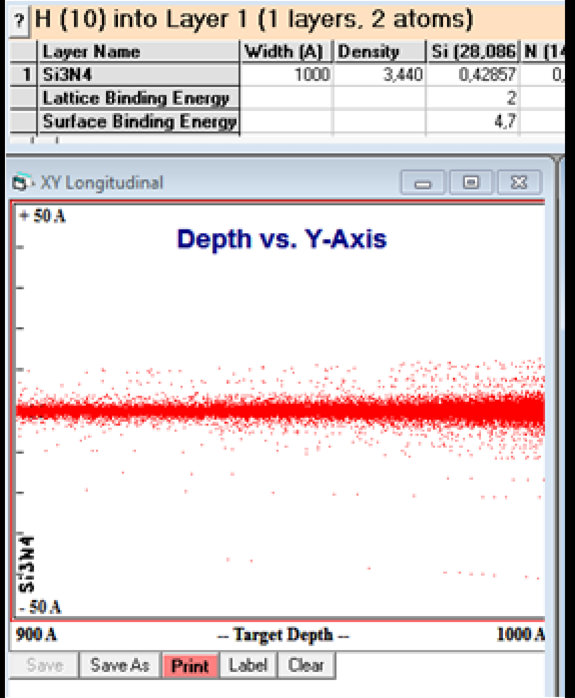


*vs*

*750 nm Al*

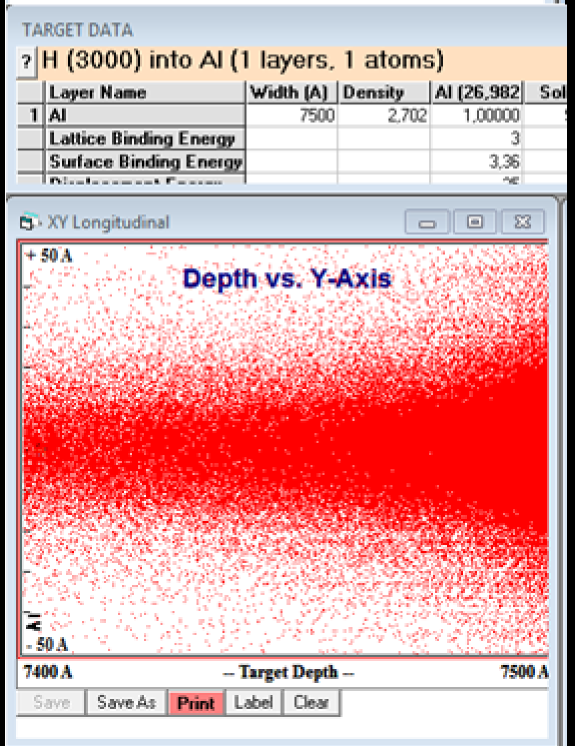


*(trim 2008 simulations)*

H (3000) into al+he (2 layers, 3 atoms)

| | Layer Name | Width (A) | Density | Si (28,086 | N (1 |
|---|---|---|---|---|---|
| 1 | Si3N4 | 1000 | 3,440 | 0,42857 | 0 |
| 2 | he | 20000000 | 0,000179 | 0,00000 | 0 |
| | Lattice Binding Energy | | | 2 | |

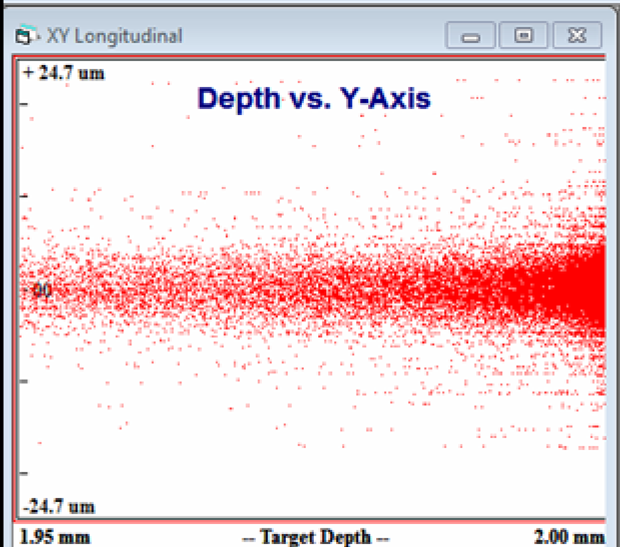


H (3000) into Layer 1+he (2 layers, 2 atoms)

| | Layer Name | Width (A) | Density | Al (26,982 | He ( |
|---|---|---|---|---|---|
| 1 | Layer 1 | 7500 | 2,702 | 1,00000 | 0 |
| 2 | he | 20000000 | 0,000179 | 0,00000 | 1 |
| | Lattice Binding Energy | | | 3 | |

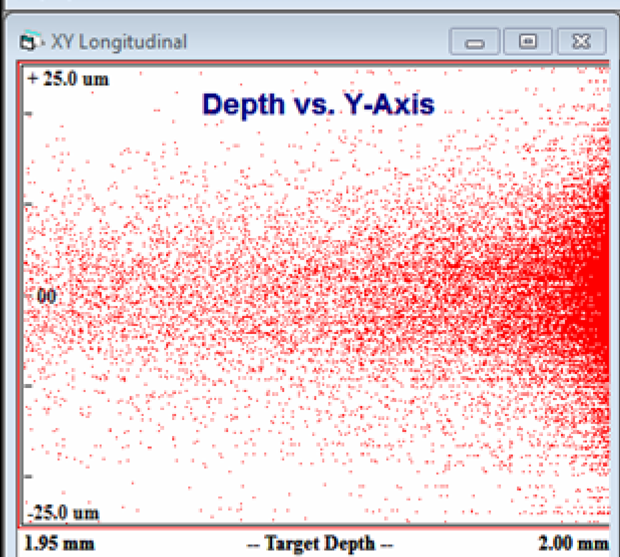


100 nm $Si_3N_4$ windows + 2 mm He

vs

750 nm Al windows + 2 mm He

# $Si_3N_4$ windows + atmosphere (air or He)

(SRIM 2008 simulations)

| Path lenght in atmosphere | Energy loss | | *Straggling($\sigma$)* | |
|---|---|---|---|---|
| | Air | He | Air | He |
| 2 mm | 28 keV | 6 keV | 4 keV | 1.5 keV |
| 3 mm | 40 keV | 8 keV | 5 keV | 2 keV |
| 4 mm | 54 keV | 10 keV | 6 keV | 2 keV |

| Path lenght in atmosphere | FWHM | | FW1/100M | |
|---|---|---|---|---|
| | Air | He | Air | He |
| 2 mm | ~6 μm | ~3.5 μm | ~25 μm | ~14 μm |
| 3 mm | ~11 μm | ~5 μm | ~50 μm | ~21 μm |
| 4 mm | ~18 μm | ~7 μm | ~74 μm | ~30 μm |

# External set-up: micron resolution is a limit?

*Sample contribution*

| path lenght in the sample | FWHM | FW1/100M |
|---|---|---|
| 10 μm | ~0.3 μm | ~1.5 μm |
| 20 μm | ~0.7 μm | ~4 μm |
| 30 μm | ~2 μm | ~8 μm |
| 40 μm | ~3 μm | ~10 μm |

(3 MeV protons in a medium Z sample (Pyrite) 3 MeV; *range* = 40 μm )

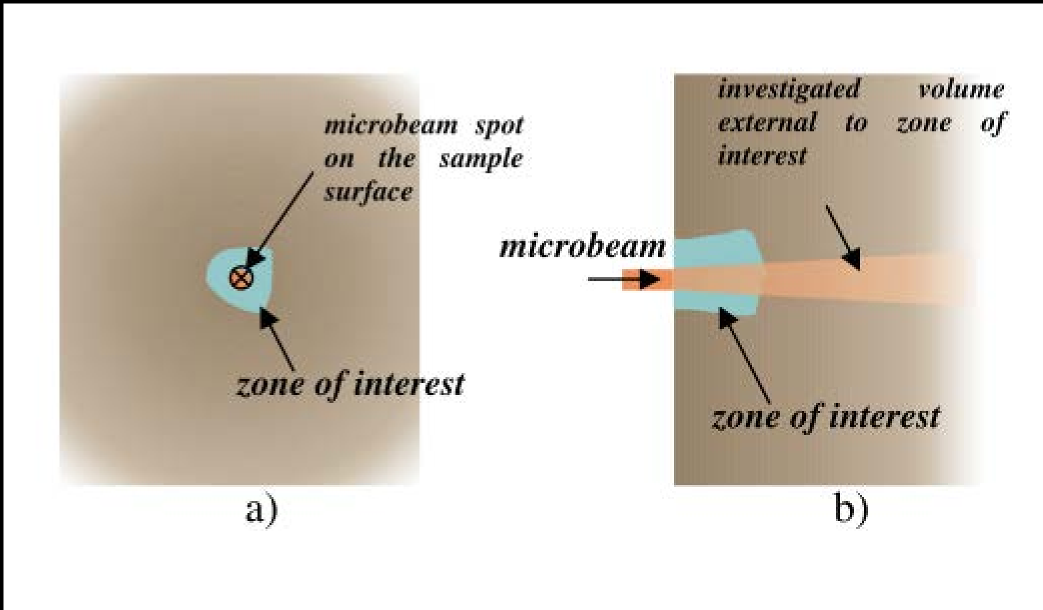


**Fig. 1** (**a**) Zone of interest of the sample and beam spot (top view); (**b**) beam penetrating into the sample (cross sectional view), investigating a layer thicker than the zone of interest

# External set-up: $Si_3N_4$ exit windows

- **standard microbeam measurements:**
  - **frame: 2.6 x 2.6 mm$^2$ wide, 0.2 mm thick**
  - ***membrane:*** ***– 100 nm thick***
    - ***0.5 x 0.5 mm$^2$***
    - ***1.0 x 1.0 mm$^2$***
- **wide area samples:**
  - **frame:** **– 5 x 5 mm$^2$ wide, 0.2 mm thick**
  - ***membrane:*** ***– 200 nm thick***
    - ***2.0 x 2.0 mm$^2$***
- **sub-millibeam applications:**
  - **frame:** **– 7.5 x 7.5 mm$^2$ wide, 0.2 mm thick**
  - ***membrane:*** ***– 500 nm thick***
    - ***2.0 x 2.0 mm$^2$***
    - ***3.0 x 3.0 mm$^2$***

# $Si_3N_4$ window, tem membrane, film...

**PELCO Holey Silicon Nitride Support Films for TEM**
www.tedpella.com/grids.../silicon-nitride-holey.ht... ▾ Traduci questa pagina
**Silicon nitride** support films are manufactured using state-of-the-art semiconductor and MEMS ... 1 ea **Si3N4** 15nm membrane with 9 ea 0.1x0.1mm **windows**

**Silicon Nitride Windows - Norcada**
www.norcada.com/products/nitride-windows-xray/ ▾ Traduci questa pagina
**SILICON NITRIDE** MEMBRANE **WINDOWS** FOR MICROSCOPY ... Our **silicon nitride windows** have a single square or rectangular **window** centered on either a 200µm (NX series) thickness or 500µm (QX ... Stoichiometric **Si3N4** Membranes.

**SPI Silicon Nitride Membrane Window Grids for TEM - SPI ...**
www.2spi.com/catalog/grids/silicon-nitride.php ▾ Traduci questa pagina
The SPI **Silicon Nitride** Membrane **Window** grids from SPI Supplies are the ultimate for those working with nanoparticles and conducting in situ high temperature ...

**Material: Silicon Nitride (Si3N4), film - MEMS Clearinghouse**
www.memsnet.org/material/siliconnitridesi3n4film/ ▾ Traduci questa pagina
Material: **Silicon Nitride** (**Si3N4**), film ... optical measurements, value obtained by direct measurements of composite **Si3N4**/SiO2 **windows** using load deflection ...

**Silson**
www.silson.com/ ▾ Traduci questa pagina
Standard **silicon nitride** membrane **windows**. The standard range of Silson **silicon nitride** membrane **windows** consist of square **silicon nitride** membranes in ...

**Silicon Nitride TEM Grids - TEMwindows.com**
www.temwindows.com/category_s/22.htm ▾ Traduci questa pagina
For examples of how these **Silicon Nitride** TEM **windows** can be used, please see Featured Publications. Competitively Priced: state of the art manufacturing ...

**PELCO® Silicon Nitride Support Films for TEM**
www.woomyoung.co.kr/silicon-nitride-details.htm ▾ Traduci questa pagina
**Silicon nitride** support films are manufactured using the latest, patented, ... by etching away a **window** in the silicon wafer substrate underneath the **Si3N4** ...

*So this is the end of the story: the only possible choice is the adoption of 100 nm $Si_3N_4$ exit windows!*

ELSEVIER Nuclear Instruments and Methods in Physics Research B 190 (2002) 271–275

www.elsevier.com/locate/nimb

# JAERI Takasaki in-air micro-PIXE system for various applications

Takuro Sakai [a,*], Tomihiro Kamiya [a], Masakazu Oikawa [a], Takahiro Sato [b], Akira Tanaka [b], Keizo Ishii [b]

[a] *Advanced Radiation Technology Center, Japan Atomic Energy Research Institute, 1233 Watanuki, Takasaki, Gunma 370-1292, Japan*

[b] *Department of Quantum Science and Energy Engineering, Tohoku University, Aramaki, Aoba, Sendai 980-8579, Japan*

**Abstract**

In JAERI Takasaki, an in-air micro-PIXE system has been developed. This system enables multi-elemental mapping of samples in atmospheric environment with spatial resolution of 1 μm.

# 1 μm spatial resolution with a 4 μm Mylar window at Jaeri Takasaki

A beam exit window, which separates samples from a high vacuum beam line, is essentially required to extract scanning micro-probe. Thin organic film is an ideal material for this purpose, because it is composed by light elements and has good physical properties. A 4 μm thick Mylar foil is mainly used for the window. The foil also plays a role of sample backing to minimize the distance between the window and samples. A sketch of the external beam apparatus for micro-PIXE is shown in Fig. 1. The window is attached on each sample holder, which is an annular disk made by acrylic resin and the tapered hole has a 1 mm diameter on the atmospheric side. Samples are set on the holders and can be observed by an optical microscope (KEYENCE VH-6300) even during irradiation. Up to six holders can be mounted on the revolving stage. A carbon coated 100 μm thick Mylar foil is attached in front of the microscope as the beam dump. The final resolution of the extracted proton beam can be kept nearly 1 μm

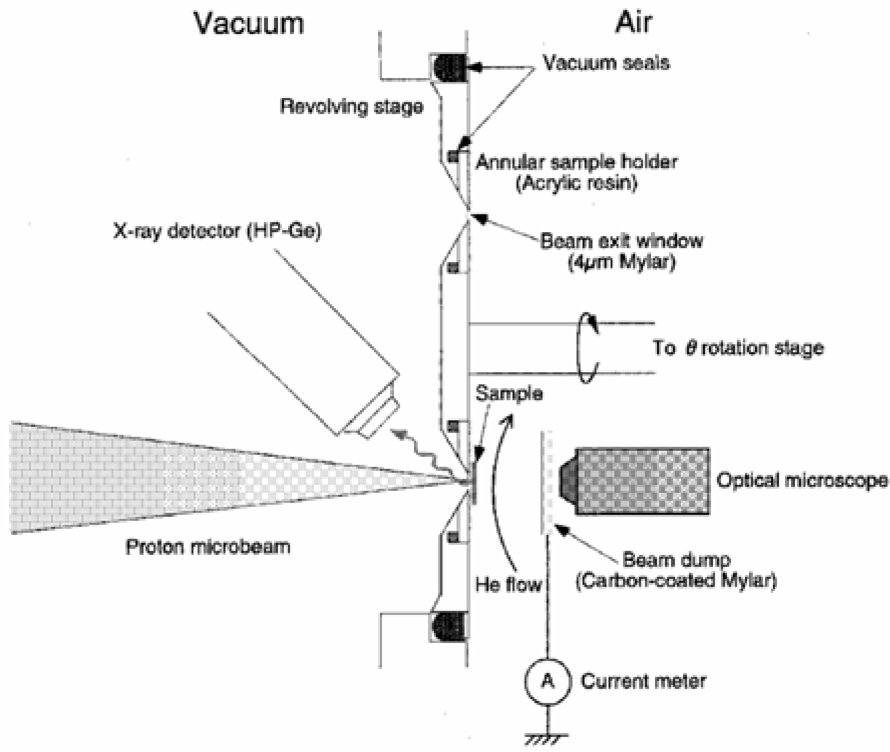


Fig. 1. Cross-sectional view of an external micro-beam apparatus for micro-PIXE analysis.

# *Wakasa Wan external microbeam facility*

Nuclear Instruments and Methods in Physics Research B 269 (2011) 2180–2183

## Progress of in-air microbeam system at the Wakasa Wan Energy Research Center

K. Yasuda [a,*], M. Nomachi [b], Y. Sugaya [b], H. Yamamoto [c], H. Komatsu [d]

[a] *The Wakasa Wan Energy Research Center, 64-52-1 Nagatani, Tsuruga, Fukui 914-0192, Japan*
[b] *Graduate School of Science, Osaka University, 1-1 Machikaneyama, Toyonaka, Osaka 560-0043, Japan*
[c] *Graduate School of Dentistry, Osaka University, 1-8 Yamadaoka, Suita, Osaka 565-0871, Japan*
[d] *Graduate School of Dental Medicine, Hokkaido University, Kita-13, Nishi-7, Kita-ku, Sapporo 060-8586, Japan*

A R T I C L E I N F O

*Article history:*
Available online 26 February 2011

*Keywords:*
External beam
Micro-PIGE
Micro-PIXE

A B S T R A C T

Modifications of an in-air microbeam system at the Wakasa Wan Energy Research Center designed to improve its performance are described. In the previous setup, a silicon nitride membrane (area: $1 \times 1$ mm$^2$; thickness: 100 nm) was used for the beam exit window and the distance between the window and the sample was restricted to $\geqslant$1.7 mm. Due to this restriction, the beam spot size obtained using the previous setup was $13 \times 13$ μm$^2$. To reduce the beam spot size, the beam exit window was replaced by a silicon nitride membrane (area: 3 (horizontal) $\times$ 2 (vertical) mm$^2$; thickness: 200 nm). In this setup, the sample can be moved as close as 0.7 mm to the window, enabling a beam spot size of $7 \times 6$ μm$^2$ to be

# *Wakasa Wan external microbeam facility*

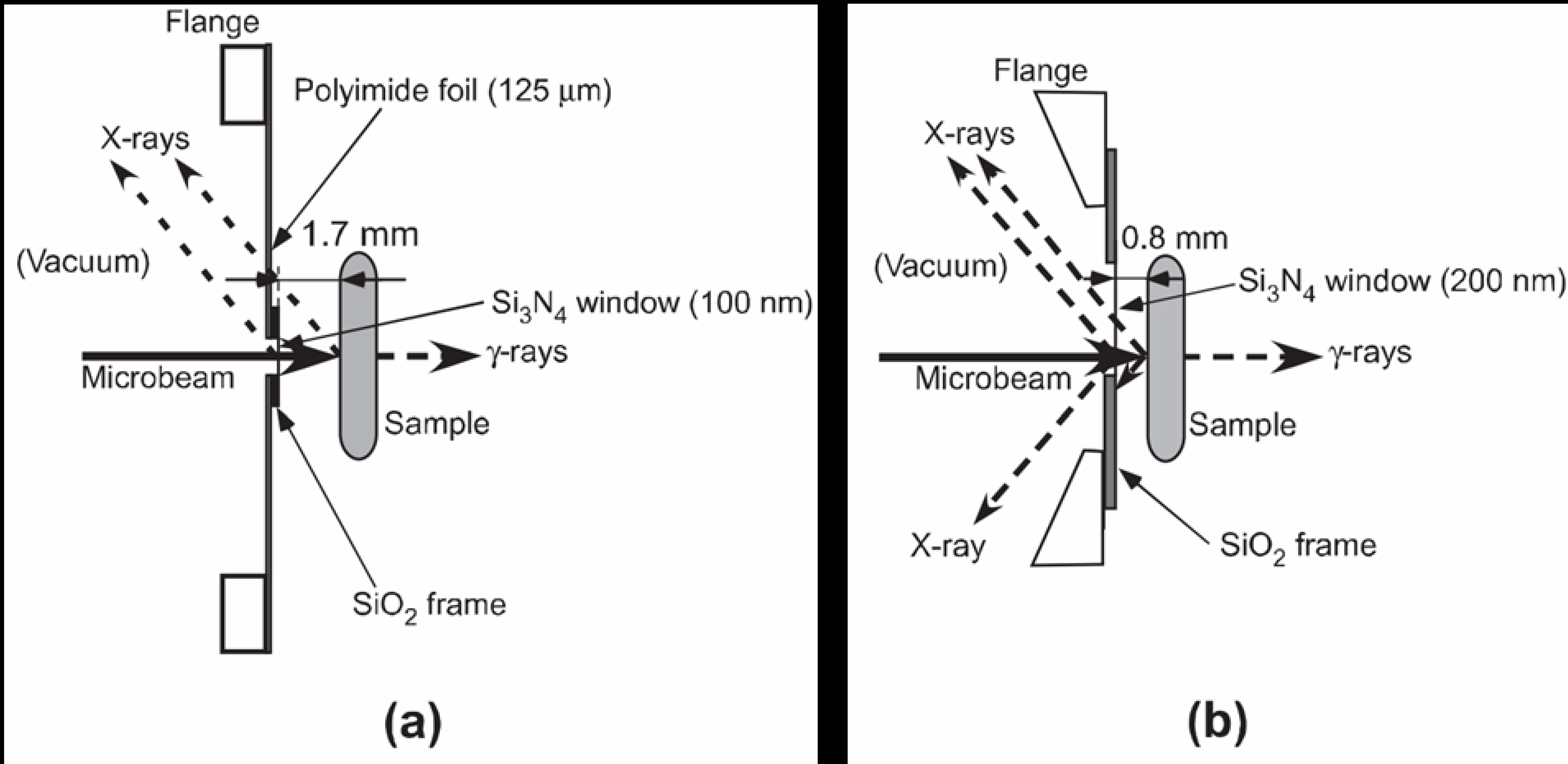


**Fig. 2.** Enlargement of beam exit region (a) previous and (b) modified setups.

# *Wakasa Wan external microbeam facility*

Since the silicon nitride membrane is much thinner than the polyimide foil, the detection efficiency of P-$K_\alpha$ X-rays increased from less than 0.01% to 54%.

The beam size was determined to be $x \times y = 7 \times 6\ \mu m^2$ (FWHM). The present beam size is approximately two times smaller than that obtained using the previous setup.

# *External microbeam with glass capillary*

ELSEVIER Nuclear Instruments and Methods in Physics Research B 249 (2006) 226–229
www.elsevier.com/locate/nimb

## In-air PIXE analysis by means of glass capillary optics

Takuya Nebiki, M. Hasnat Kabir, Tadashi Narusawa *

*Kochi University of Technology, Tosa-Yamada, Kochi 782-8502, Japan*

Available online 11 May 2006

**Abstract**

A novel technique to introduce high energy ion beams to atmospheric environment is presented, which enables in-air PIXE measurements. Slightly tapered glass capillary optics is applied to work as a differential pumping orifice as well as a focusing lens. The flux intensity is enhanced by at least one order of magnitude due to the focusing effect. Using capillaries of 10–20 μm outlet diameters, we obtain several hundreds pA of 4 MeV $He^{2+}$ ion beam and apply it to PIXE analysis of the seabed sludge without any sample treatments.

# *External beam with metal capillary*

Nuclear Instruments and Methods in Physics Research B 269 (2011) 1023–1025

## Development of two-dimensional mapping technique by in-air-PIXE with metal capillary

N. Fujita [a,*], K. Ishii [b], H. Ogawa [b]

We have developed the two-dimensional mapping technique with in-air-PIXE (2D-PIXE) using a metal capillary as a guide to extract ion beam to air. The metal capillary is the conventional injection needle with a 200 μm inside diameter. For the target which is the character made of the copper wires on aluminum basement, 2D-PIXE measurements were performed by irradiating 3 MeV proton beam. As a result, the character was tend to be restored clearly by this method. We discuss about the result of the two-dimensional map from a viewpoint of the signal-to-noise ratio and the resolution. This technique is expected to be applicable to various fields such as biology, nano-technology, archeology and so on.

# *External beam with metal capillary*

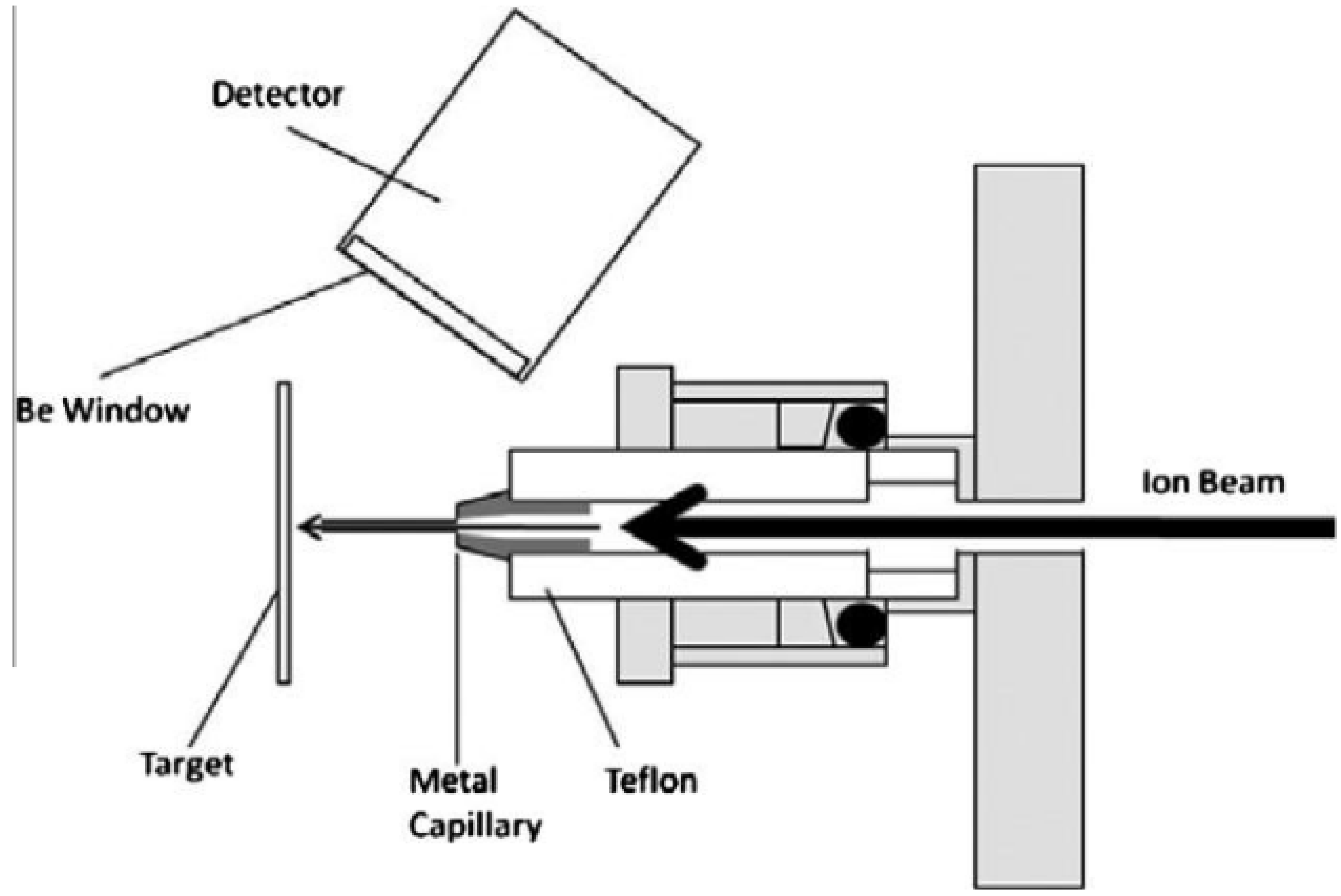


**Fig. 1.** Schematic diagram of in-air 2D-PIXE setup.

# External microbeam with metal capillary

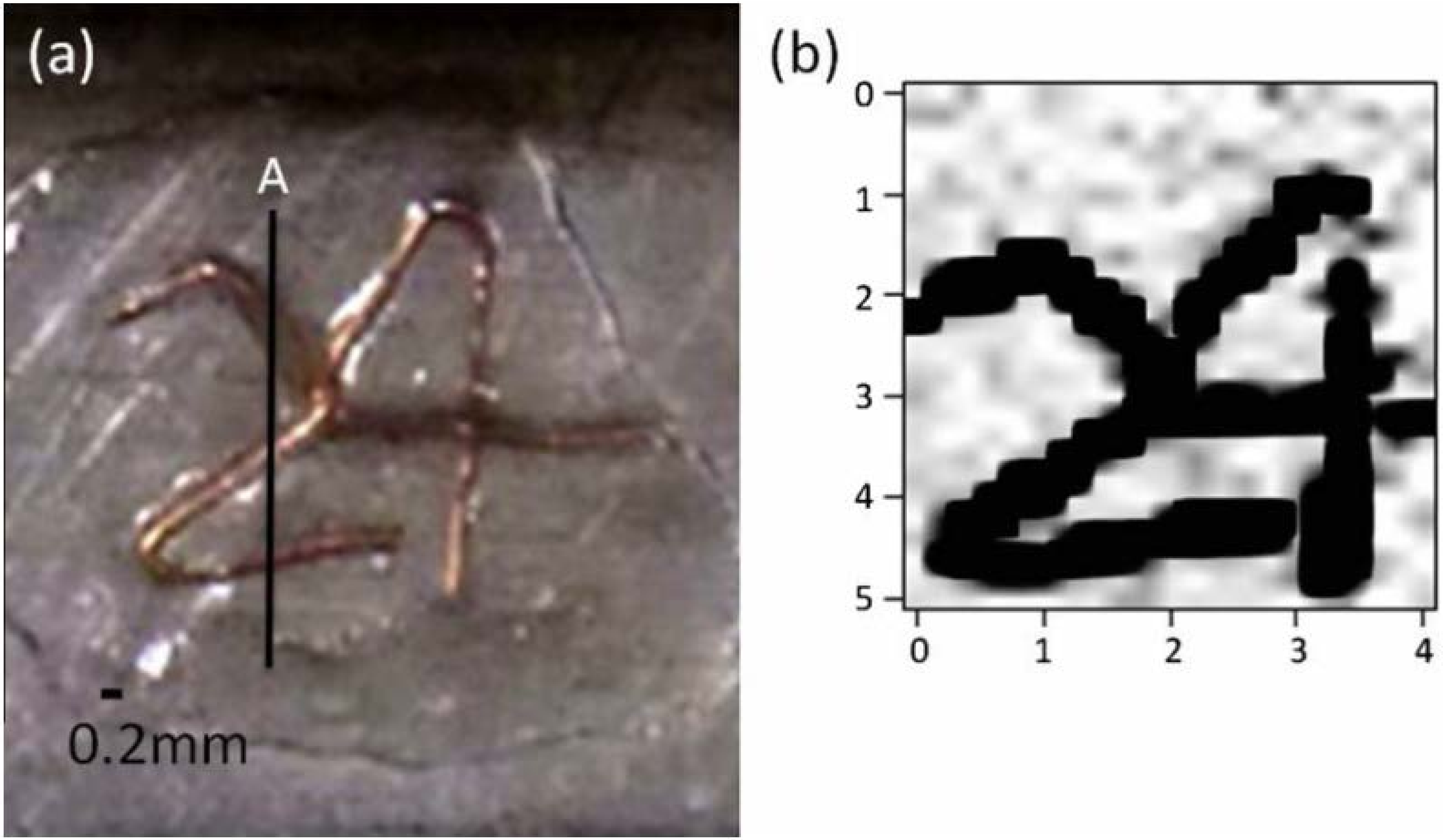


**Fig. 2.** (a) Photo of the target. (b) The result of 2D-PIXE by the characteristic X-ray of Cu.

# External microbeam at the AGLAE external microbeam 1 - 1998

*T. Calligaro et al. / Nucl. Instr. and Meth. in Phys. Res. B 136–138 (1998) 339–343*

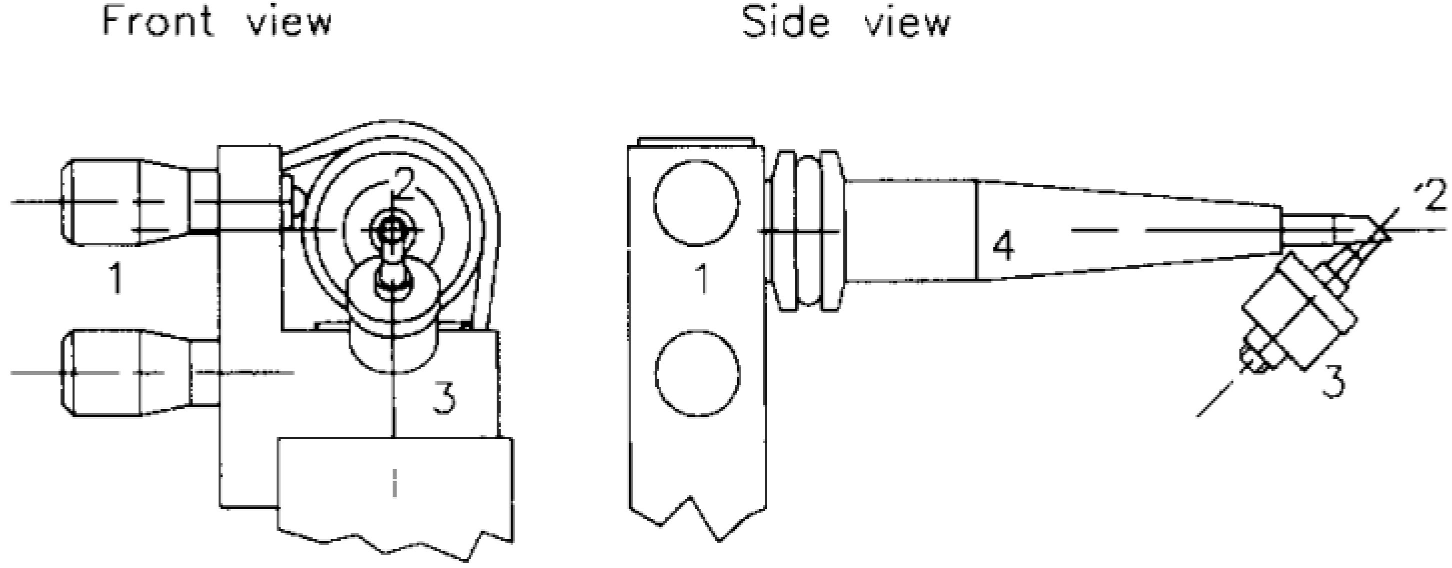


Fig. 1. Simplified sketch of an exit nozzle: (1) $x$-$y$ micrometric stage for positioning the beam at the center of the exit foil; (2) Exit foil; (3) Beam monitoring device via RBS; (4) Teflon insulating tube (necessary for beam monitoring).

0.75 µm thick Al foil supported by a 150 µm thick sapphire wafer with a 100 µm diameter hole.

# *External microbeam at the AGLAE 2 - 2000*

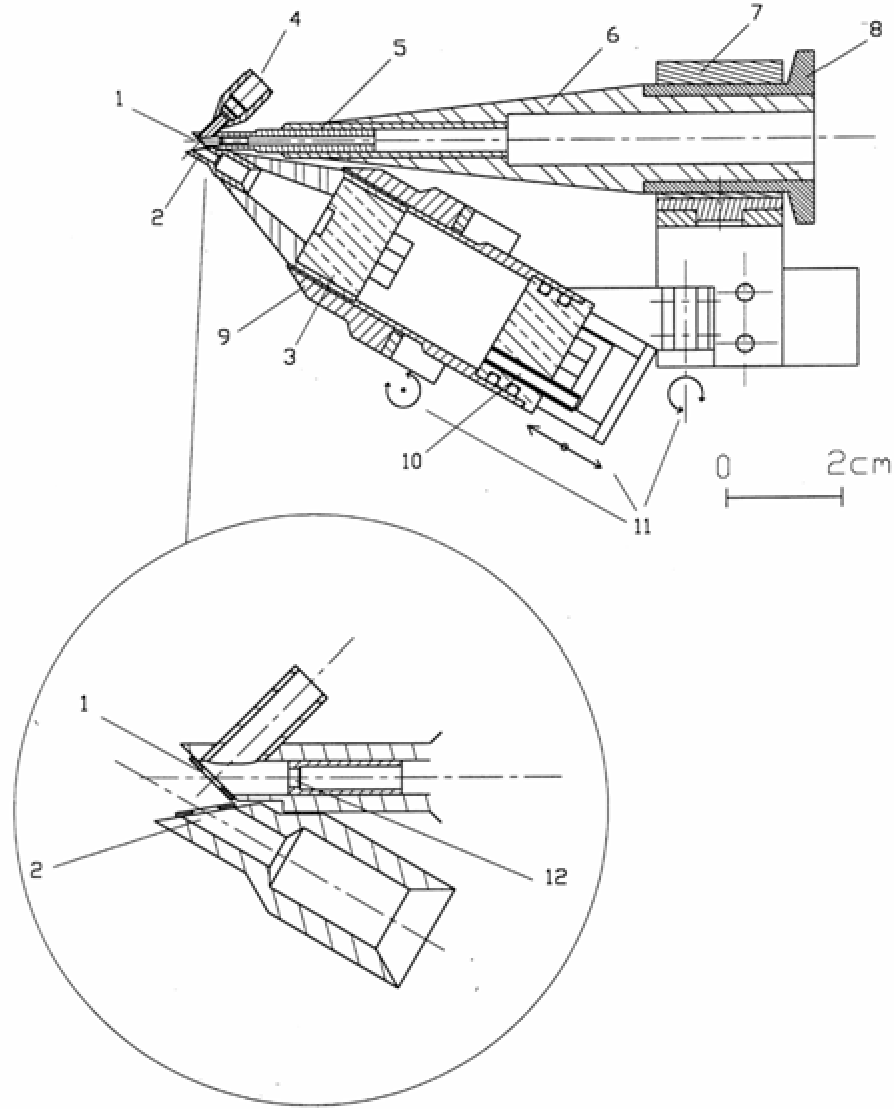


Fig. 1. Sketch of the last version of the exit nozzle for the production of an external beam. The overall length is 110 mm. The numbered parts are the following: (1) 0.1 μm $Si_3N_4$ exit foil set at 45° with respect to the beam; (2) 0.1 μm $Si_3N_4$ foil closing the detector housing; (3) Surface barrier detector set under vacuum with adjustable distance to sample; (4) Collimator system closed with a 8 μm Kapton foil and facing the exit window to allow beam monitoring with a Si(Li) X-ray detector; (5) 3-part aluminium canal; (6) Teflon cone; (7) Brass ring holding the detector housing; (8) Stainless steel vacuum adaptor; (9) Housing of the surface barrier detector; (10) Brass canal for pumping; (11) System for adjusting the detector position; (12) Brass collimator to suppress contribution of halo to monitoring signal.

# *External microbeam at the AGLAE 3 - 2004*

*2.3.1. Beam monitoring*

This is a difficult issue when operating in external beam mode, as the measurement of the integrated charge deposited on the target is no longer reliable. Several means have been reported in the literature including the use of a chopper, the Ar X-ray signal when operating in air, the RBS signal emitted by the exit window. We have used this last system in the earlier version of our set-up where a millimetre-sized beam was extracted through various windows (Kapton, Al, Ti or Zr). The shift toward the ultra-thin $Si_3N_4$ window made this means unfeasible because the RBS signal was too low.

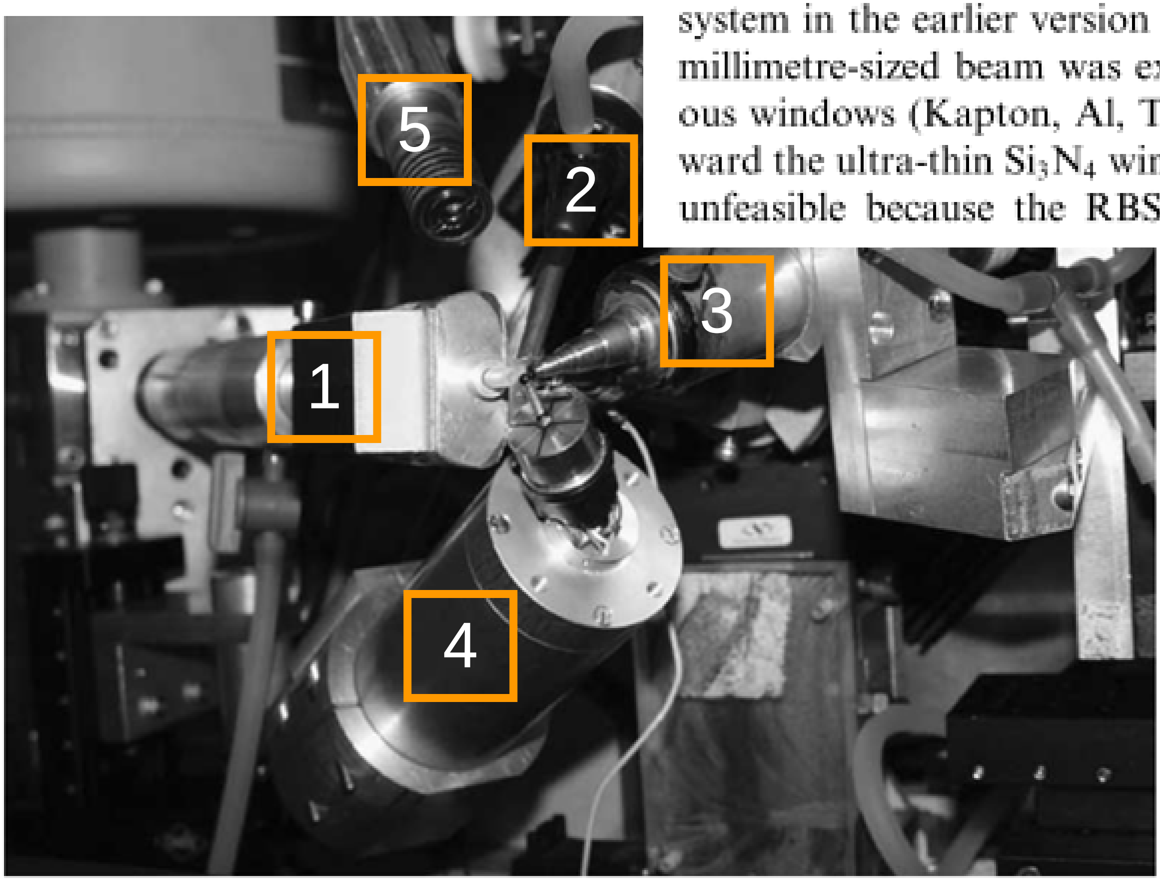


Fig. 2. Close-up view of the external beam set-up. The numbered main components are: 1. low energy X-ray Si(Li) detector equipped with a deflecting magnet; 2. high energy X-ray Si(Li) detector; 3. surface barrier detector; 4. Si-drift detector cooled by Peltier effect for dose monitoring; 5. pointing laser.

*the AGLAE external microbeam*
*4 - 2005*

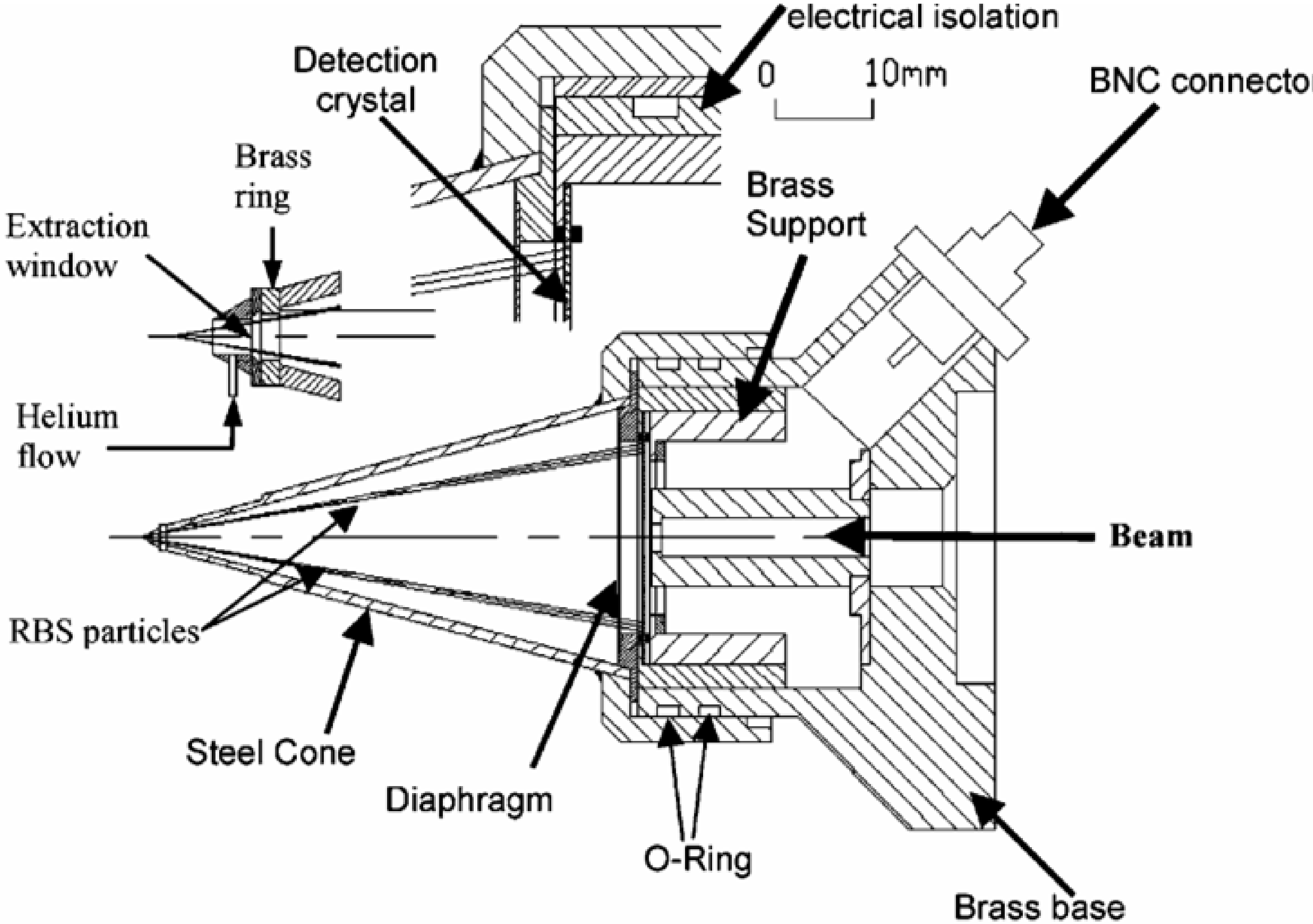


Fig. 1. Scheme of the new extracting nozzle.

*the AGLAE external microbeam 5 – 2008*

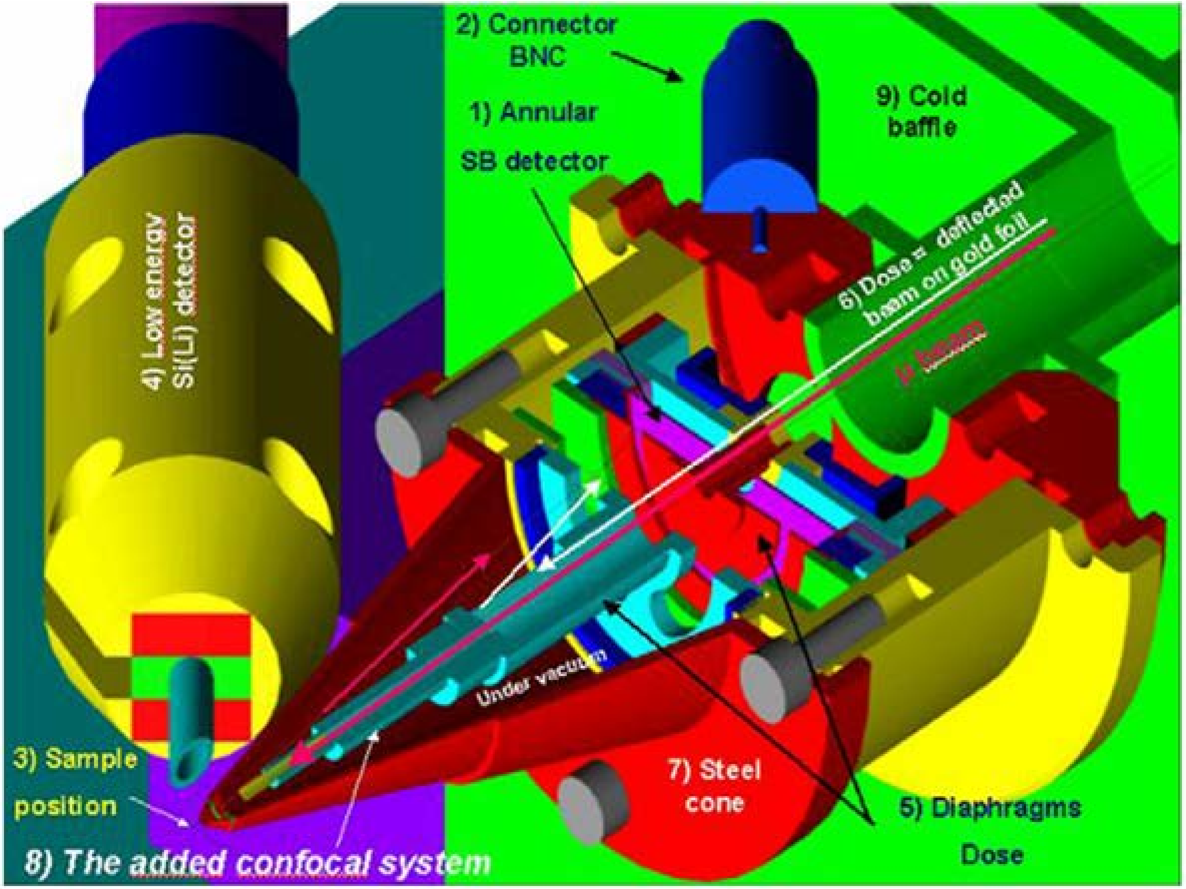


Fig. 4. Layout of the nozzle with integrated SB detector. 1-Annular SB detector. 2-BNC connector. 3-Sample position. 4-Low energy Si(Li) detector with magnetic deflector. 5-Diaphragm for dose monitoring and angle of detection definition. 6-Path of backscattered particles from sample and gold monitor. 7-Extraction steel cone. Note the new components in the latest version: 8-Collimator to suppress the signal from the exit window. 9-A cold trap in the detector housing to enhance the vacuum and reduce the content in hydrocarbides.

*the AGLAE external microbeam 4 – 2008*

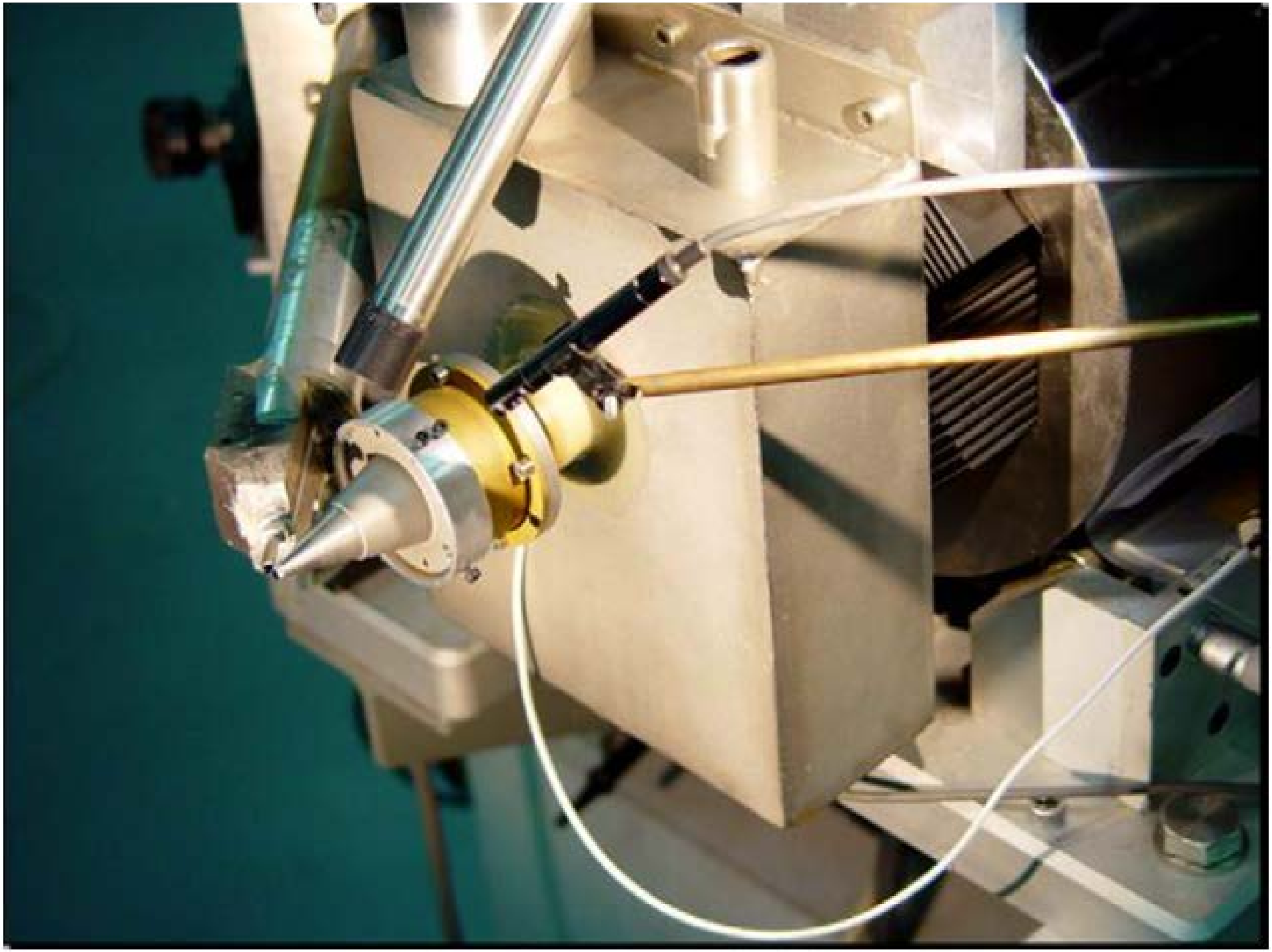

Fig. 3. The new version of the extraction nozzle which permits RBS measurement and dose monitoring, with the associated cold baffle.

# *the AGLAE external microbeam 5 – 2011*

Nuclear Instruments and Methods in Physics Research B 269 (2011) 2999–3005

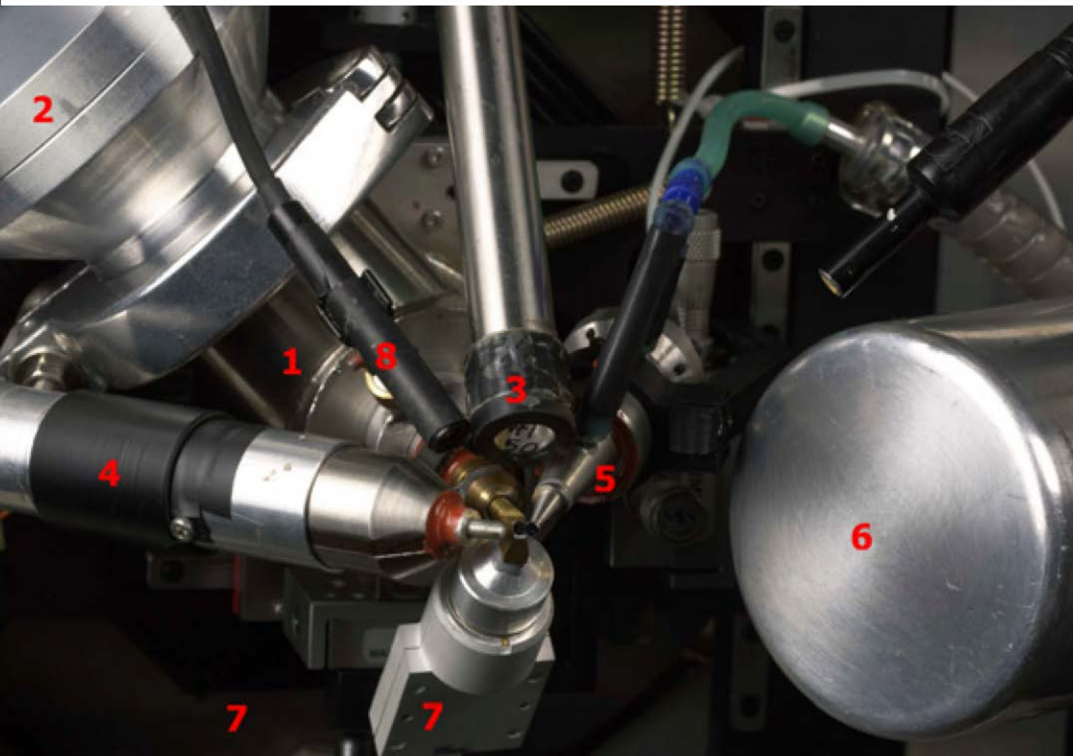


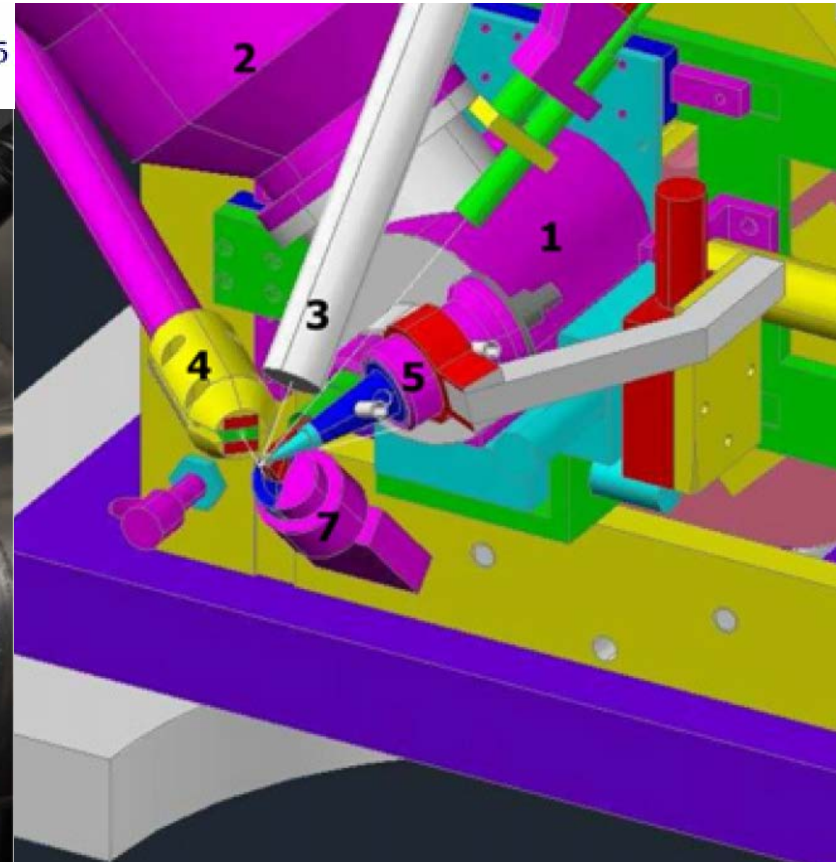


**Fig. 1.** External beam set-up used for simultaneous PIXE–RBS–PIGE. (1) Beam extraction nozzle with a $Si_3N_4$ window; (2) turbo-pump; (3) high energy Si(Li) X-ray detector equipped with a 6-µm Be window, solid angle 100 mSr; (4) low energy Si(Li) X-ray detector equipped with a deflection magnet, 0.25-µm BN window, He flux, solid angle 10 msr; (5) RBS detector; (6) gamma detector; (7) dose detector: SDD Peltier cooled detector; (8) camera for positioning.

# *the AGLAE external microbeam 6 – 2014*

*L. Pichon et al. / Nuclear Instruments and Methods in Physics Research B 318 (2014) 27–31*

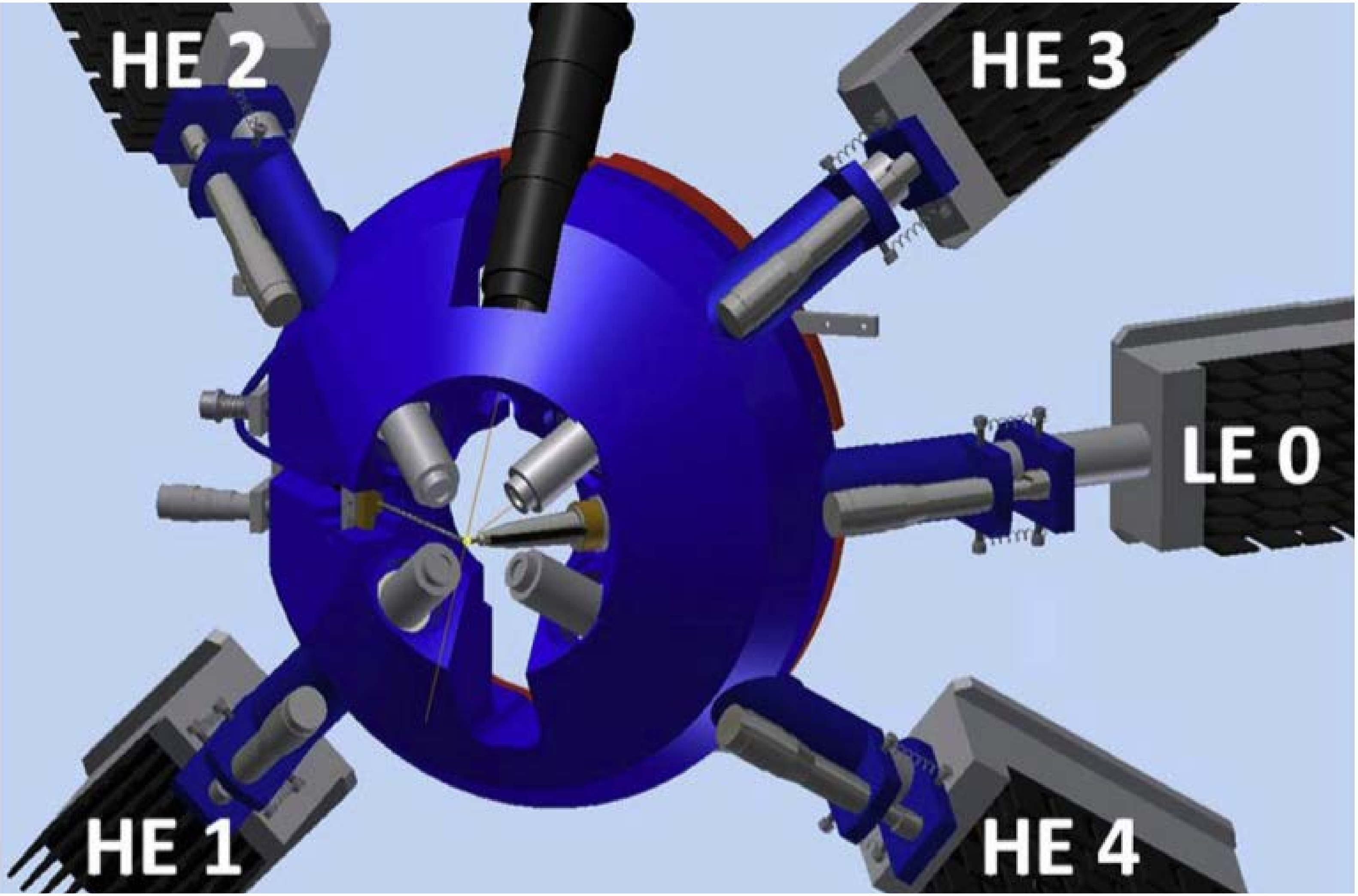


maximum solid angle for high energy detectors is $4 \times 125$ msr = 500 msr.

# LABEC PIXE-PIGE-BS measurements

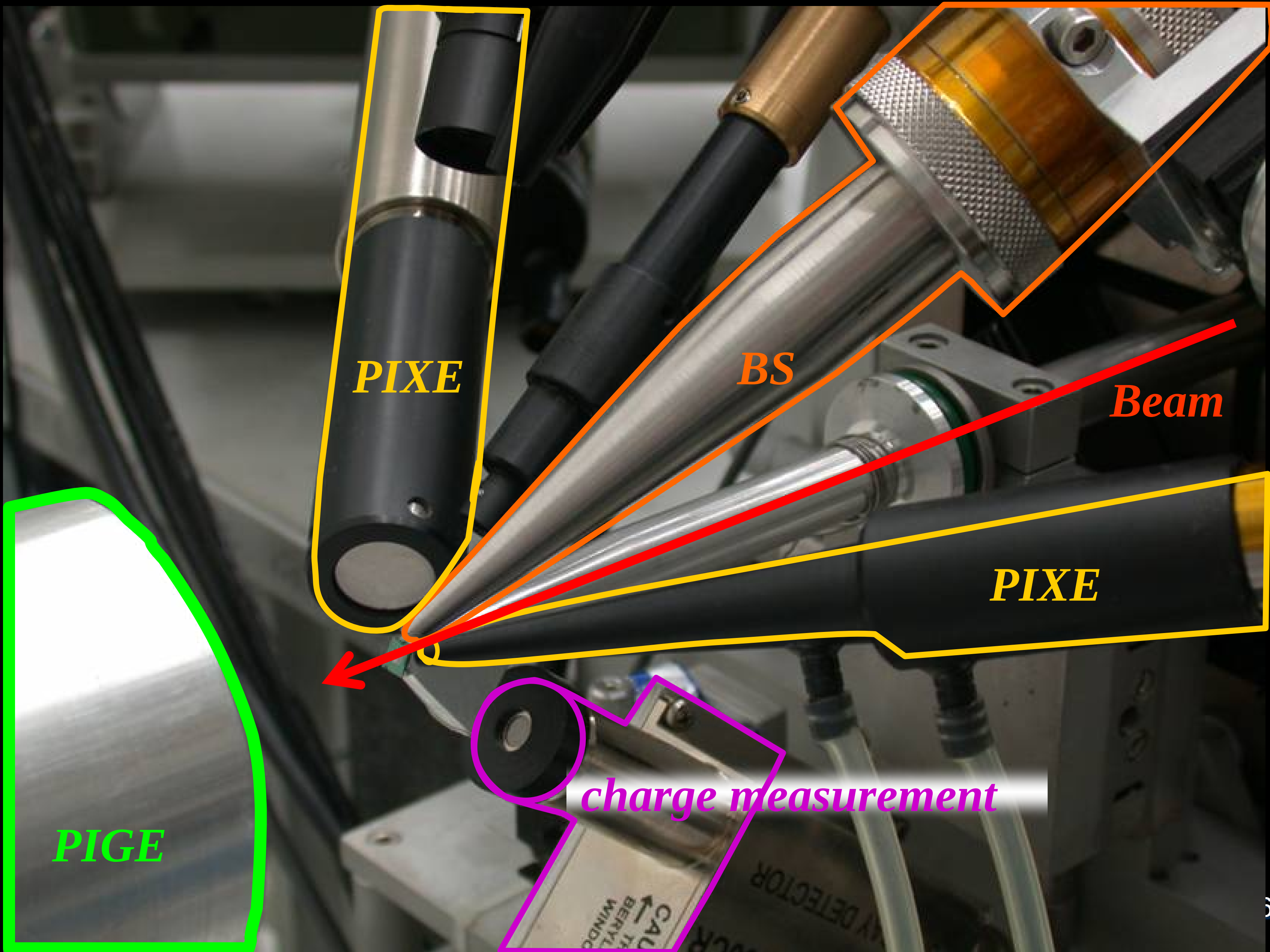

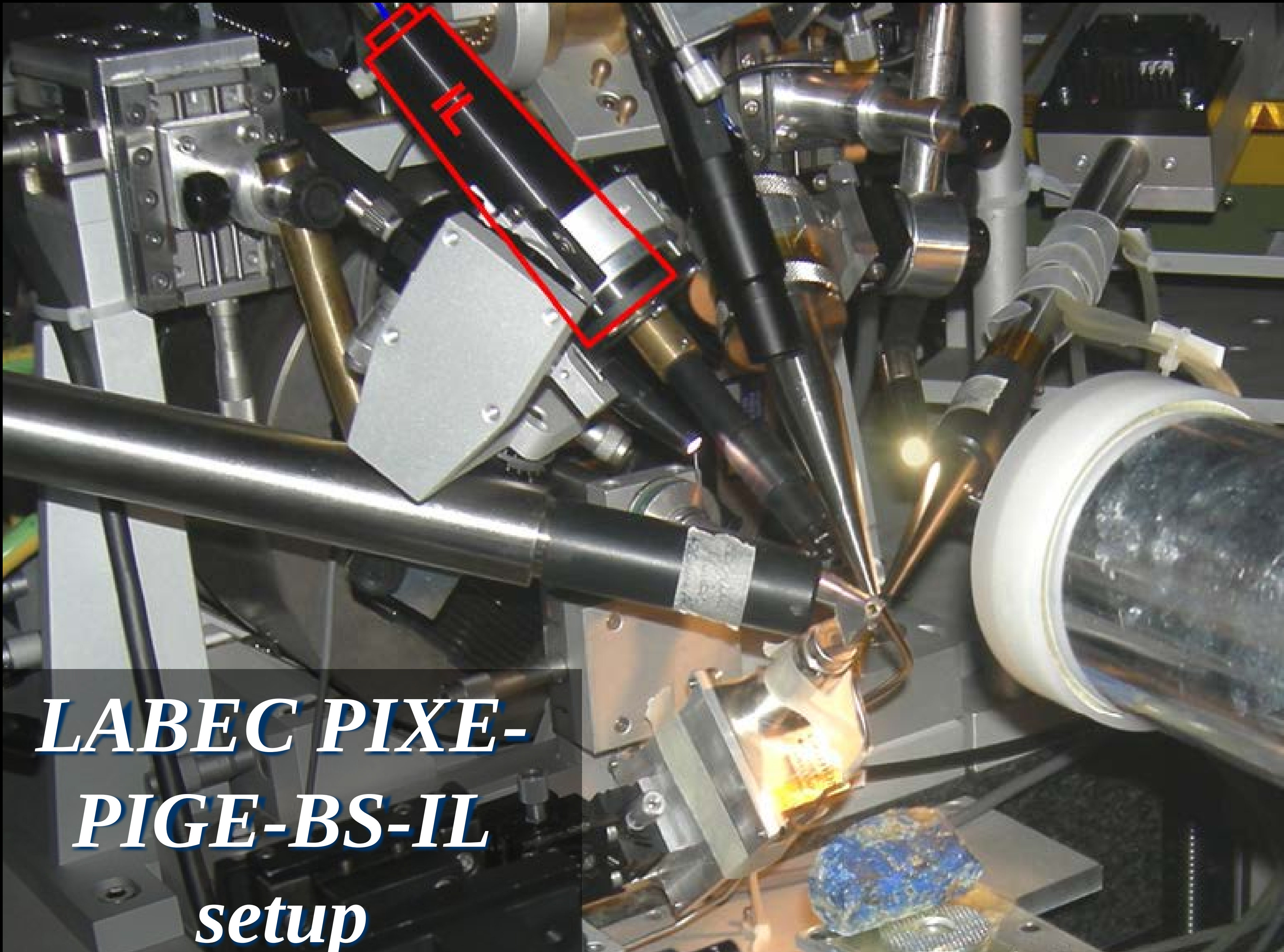
IL
LABEC PIXE-
PIGE-BS-IL
setup

*PIXE analysis of the Trivulzio portrait by Antonello da Messina*

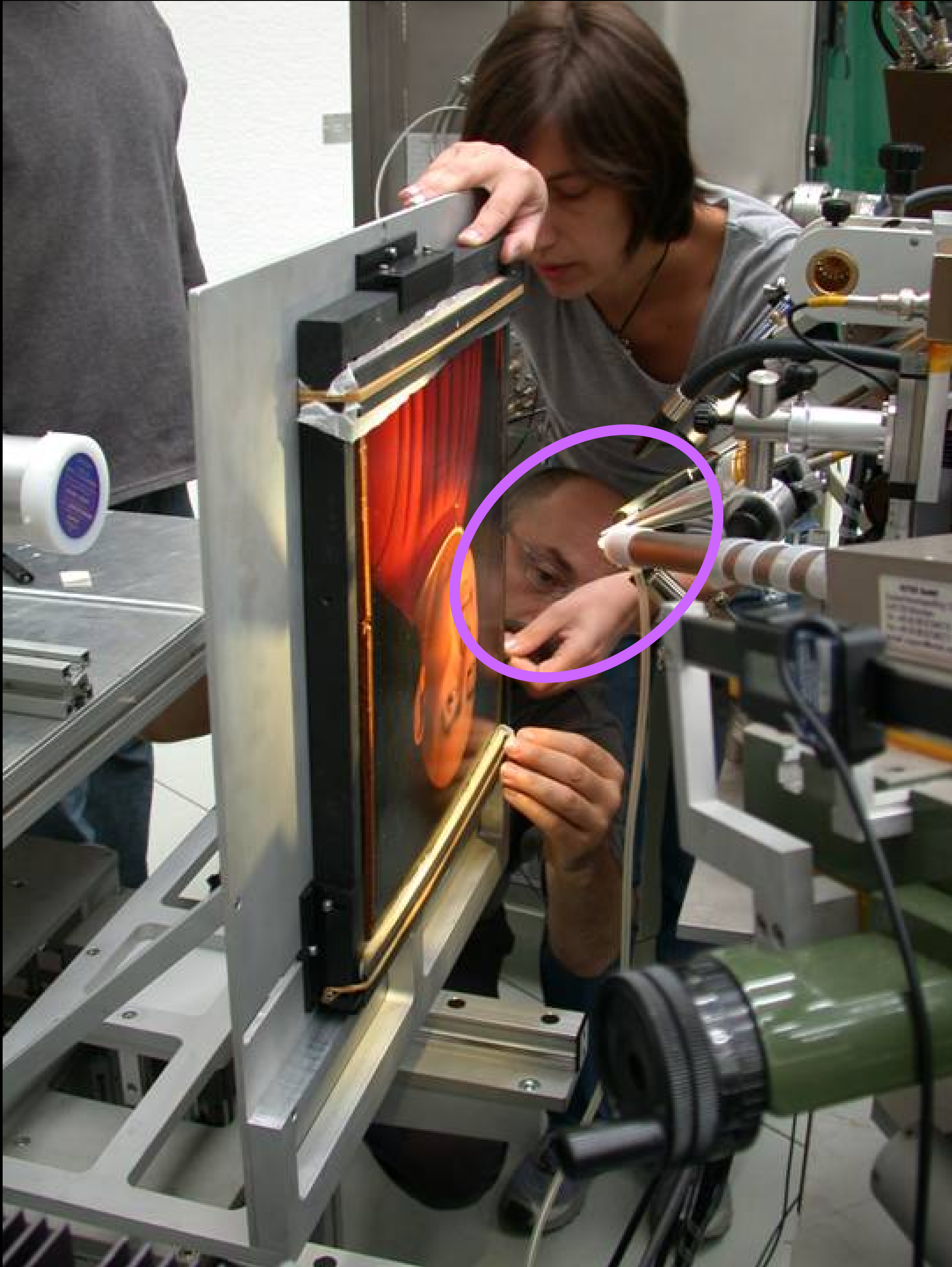

# scanning-PIXE: why?

*photograph after the removal of the old varnish*

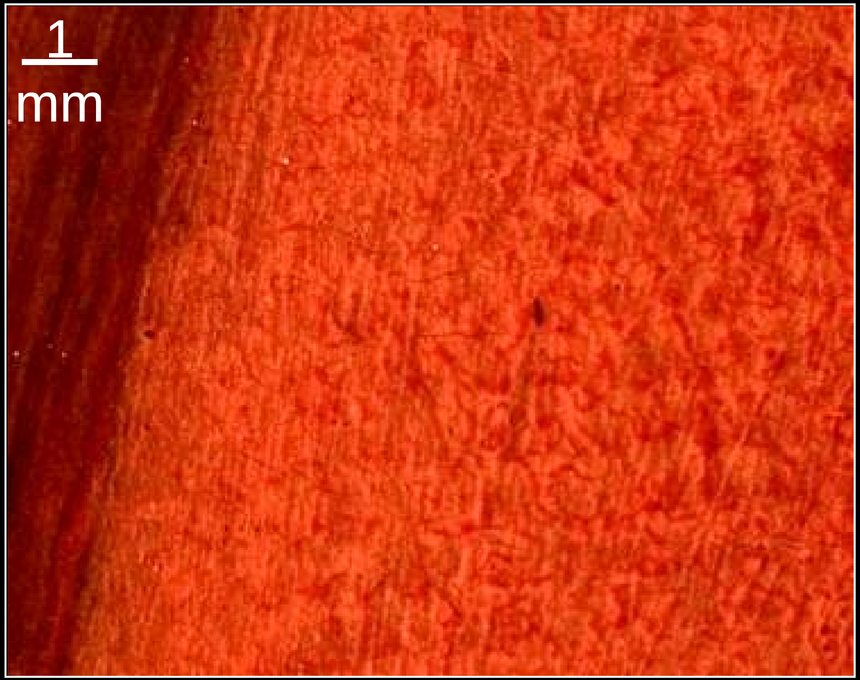


Unusual surface with darker spots with sub-millimetre dimensions

need of good spatial resolution probe and an imaging approach, in order to correlate elemental distributions to visible details

# *The red mantle*

*$E_p = 3$ MeV*

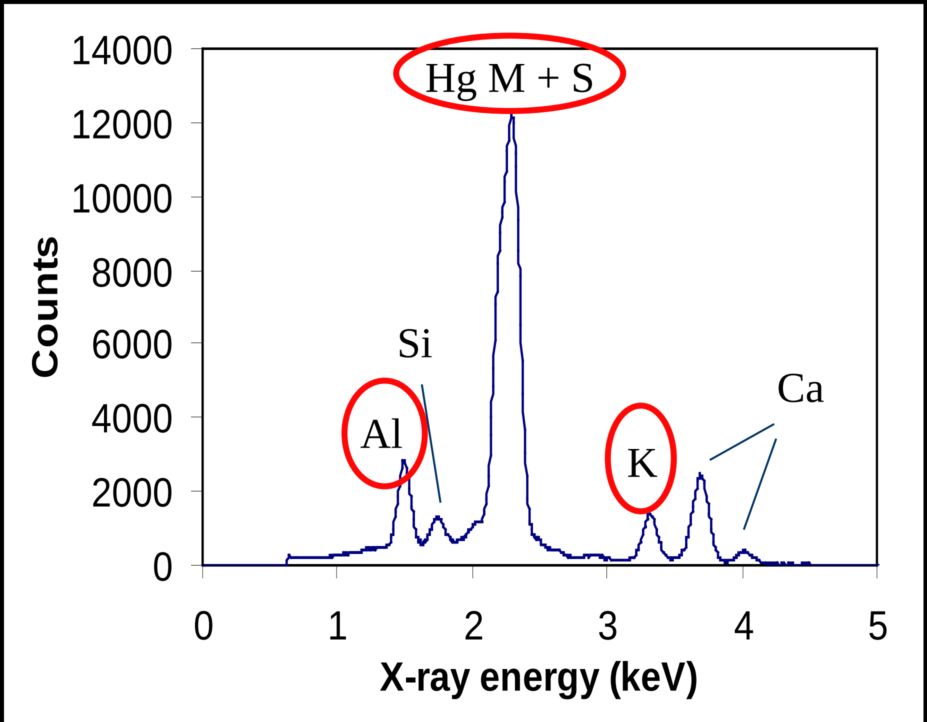


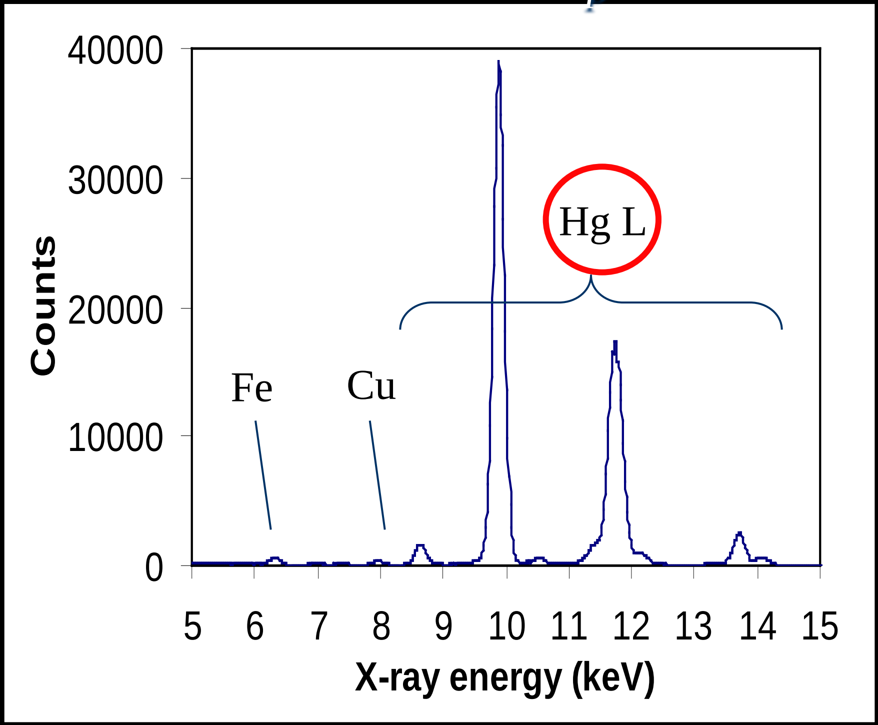


- PIXE spectra dominated by Hg and S X-ray peaks → cinnabar (HgS)
- Other elements presents (Al, K), not characteristic of a particular pigment

# Al, K and Hg

Hg M + S $K_\alpha$

$E_X \sim 2.3$ keV

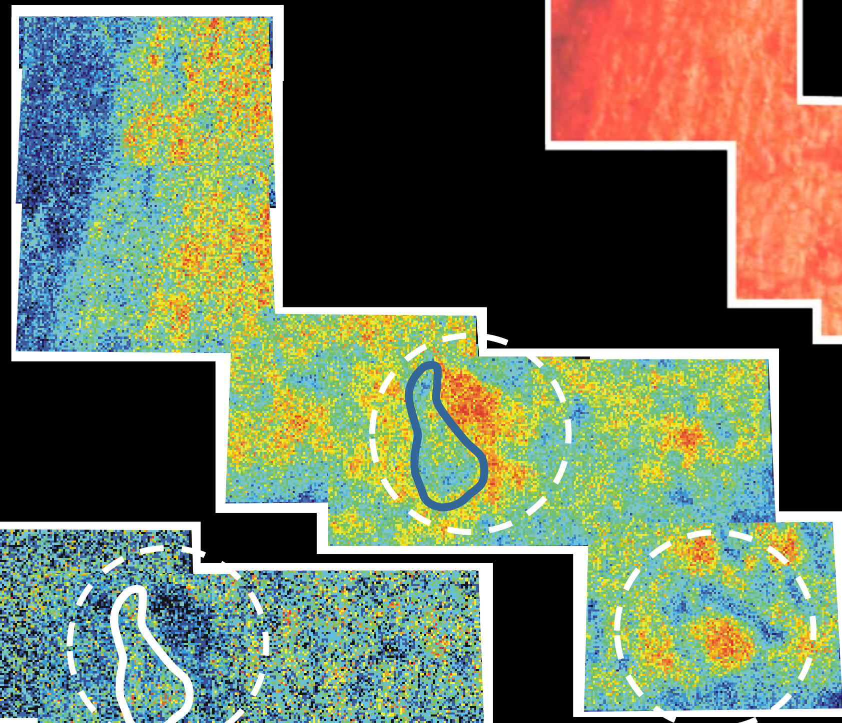

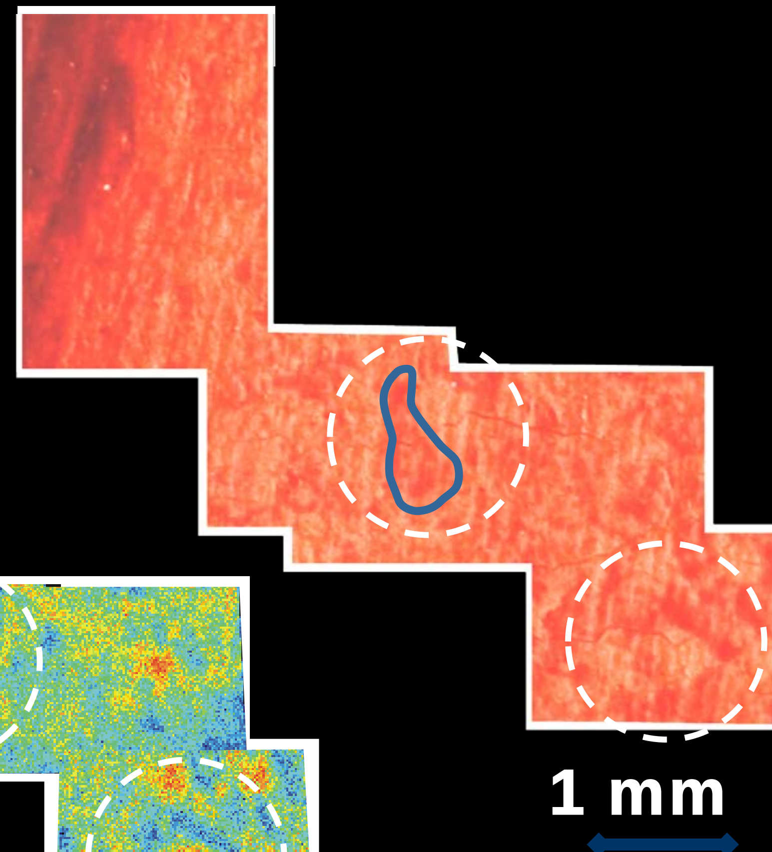


K $K_\alpha$

$E_X \sim 3.3$ keV

Al $K_\alpha$

$E_X \sim 1.5$ keV

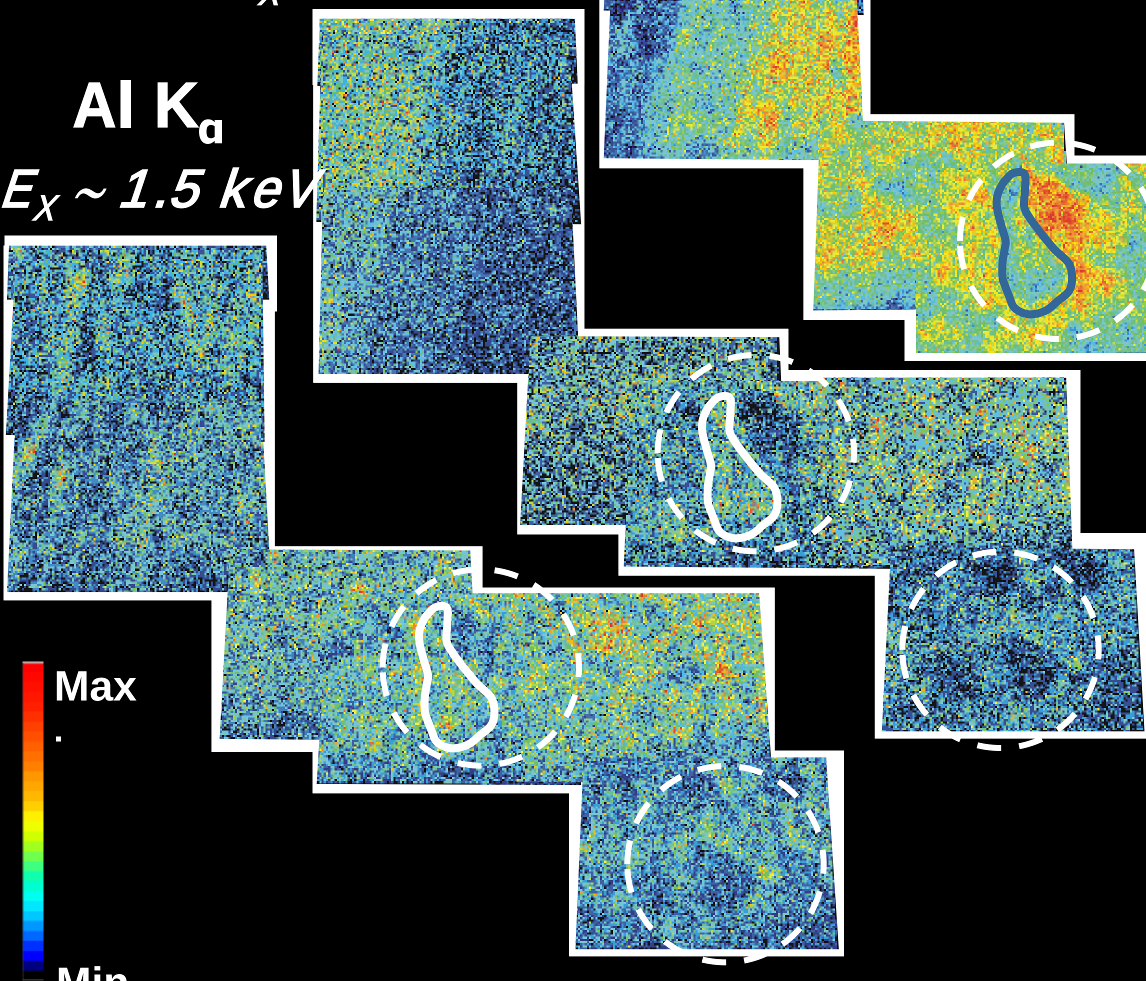


...maybe an indication for the substitution of Cinnabar (Hg +S) with a red pigment based on K and Al?

# Hg: M and L lines

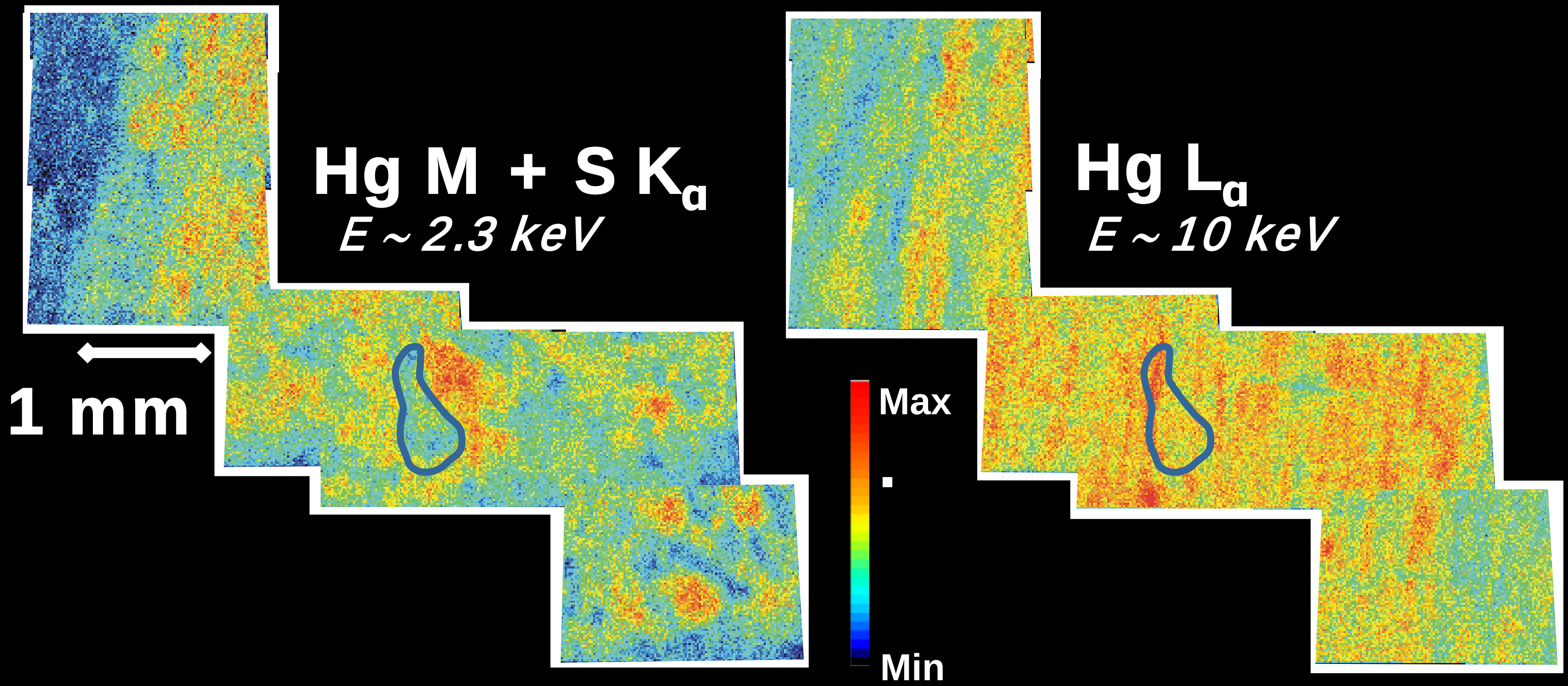


**The Hg LOW energy X rays map shows the"lack" of cinnabar**
**The Hg HIGH energy X rays map does <u>not</u> show the lack of cinnabar.**

**This effect suggests the presence of a very thin layer over the cinnabar, sufficient to absorb the low energy X rays from Hg but practically transparent for those of higher energy.**

# *Metal point drawings*

**LEONARDO DA VINCI** STUDY OF A DRAPERY
ROMA, ISTITUTO NAZIONALE PER LA GRAFICA
metal point + lead white red prepared paper

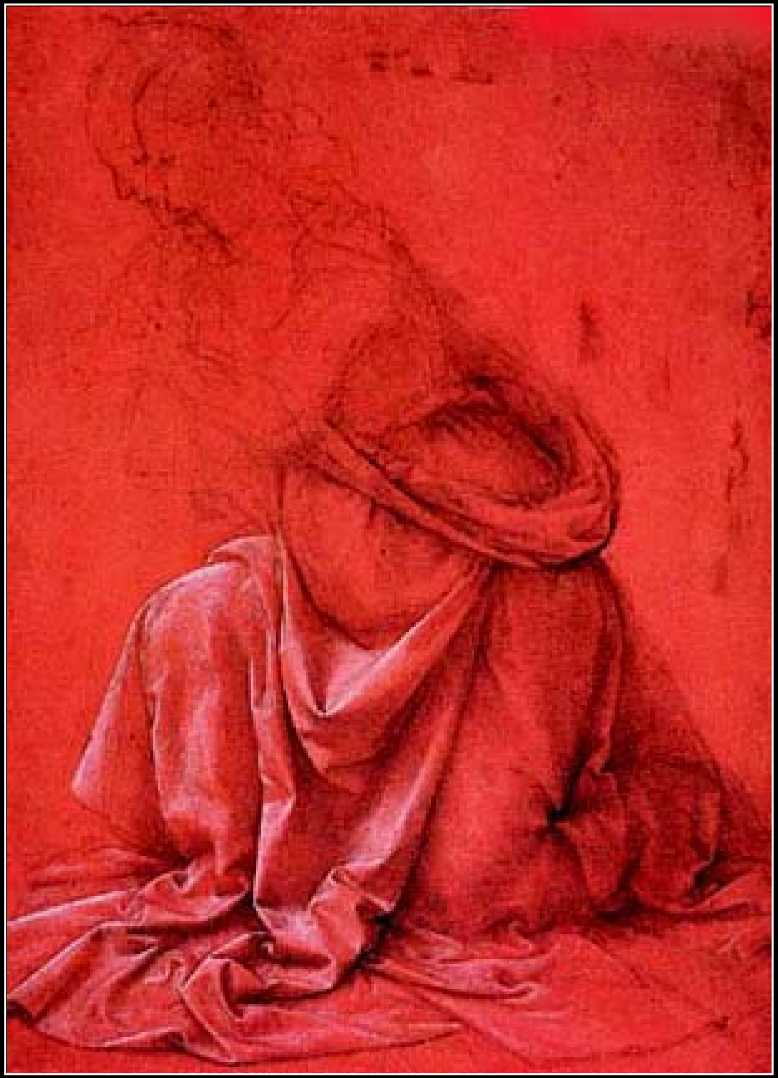

**FILIPPINO LIPPI -** STUDY
Firenze, Opificio delle Pietre Dure
metal point +  prepared paper

# Metal-point drawings on prepared paper

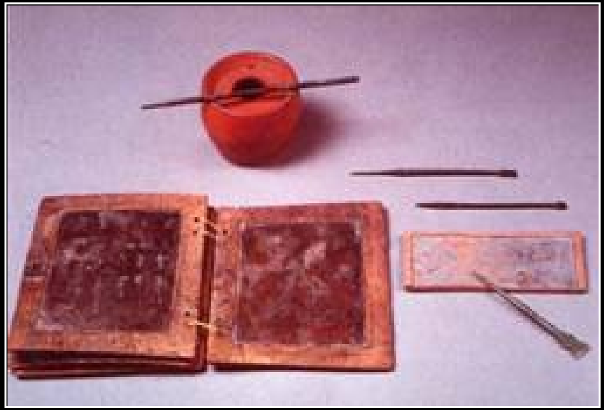

- Knowledge of materials to allow restorers to deal with fragile and precious works, so far little studied from a scientific point of view
- Problem: non uniform track of the metal stylus makes material identification difficult
- Need of *<u>a non-destructive imaging technique</u>*, spatial resolution better than 100 μm

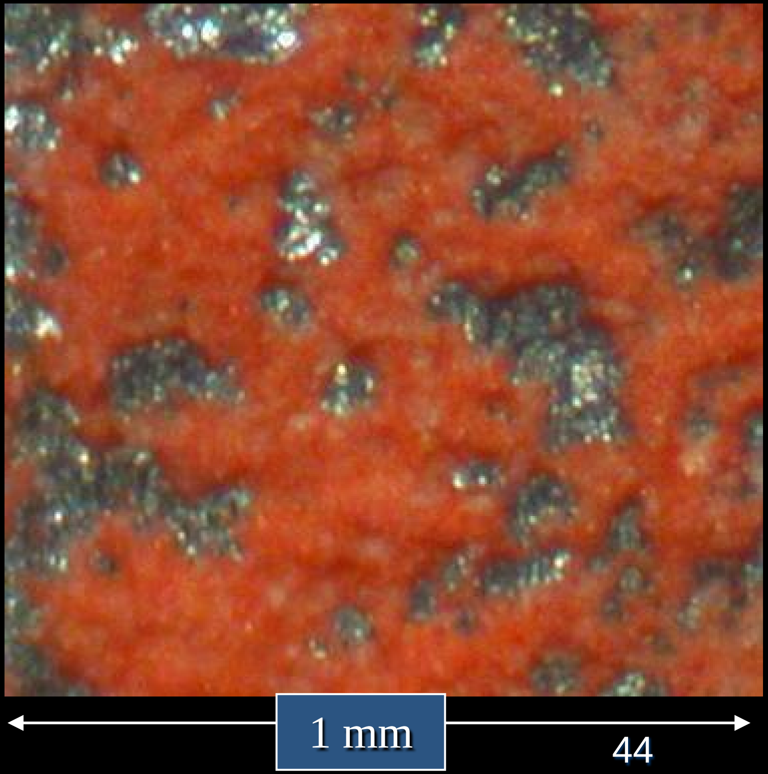

# *Example of challenging metal point drawings*

Pb stylys on
cinnabar + Pb-white
prepared paper

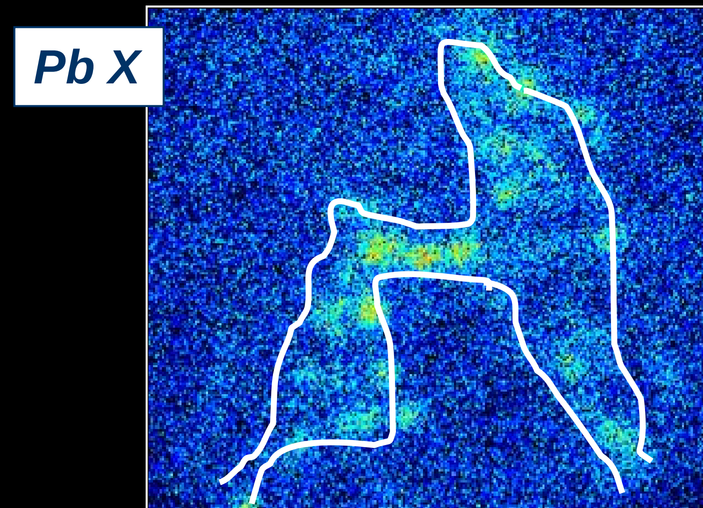


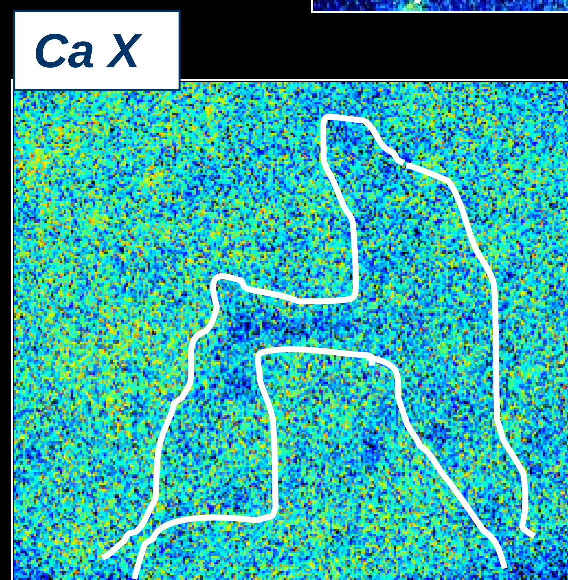


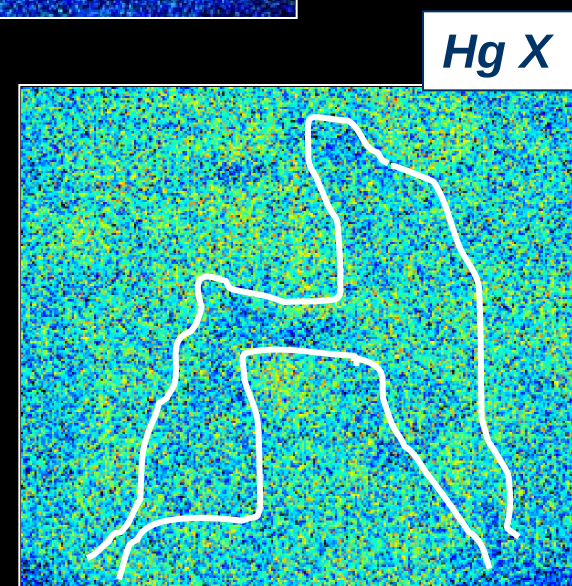

# *Results - I Mineral identification*

<u>LAZURITE</u> (*Na and S*)

<u>DIOPSIDE</u> (*Ca* e *Mg*)

**PIGE Na** **PIXE S** **PIXE Ca** **PIXE Mg**

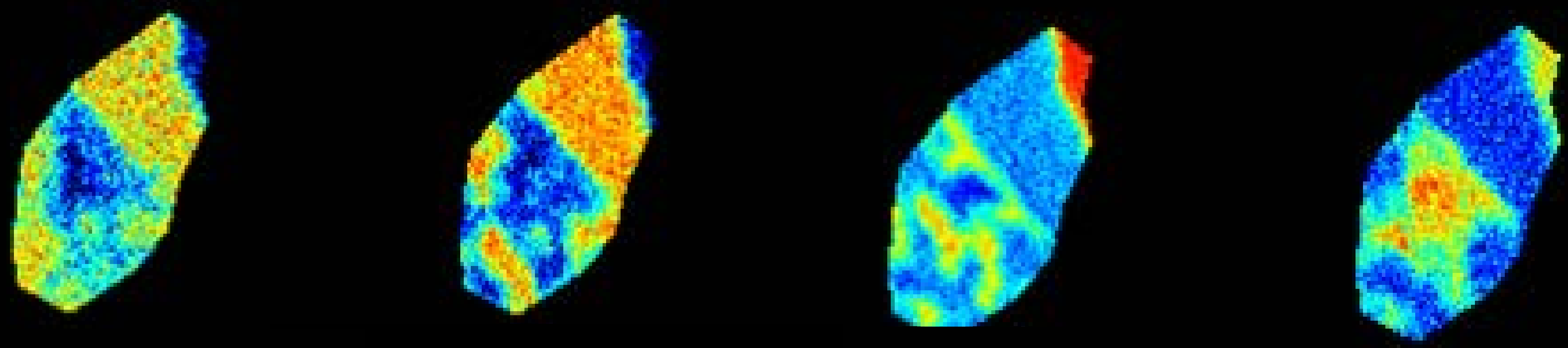

**PIXE K** **PIGE F** **IL**

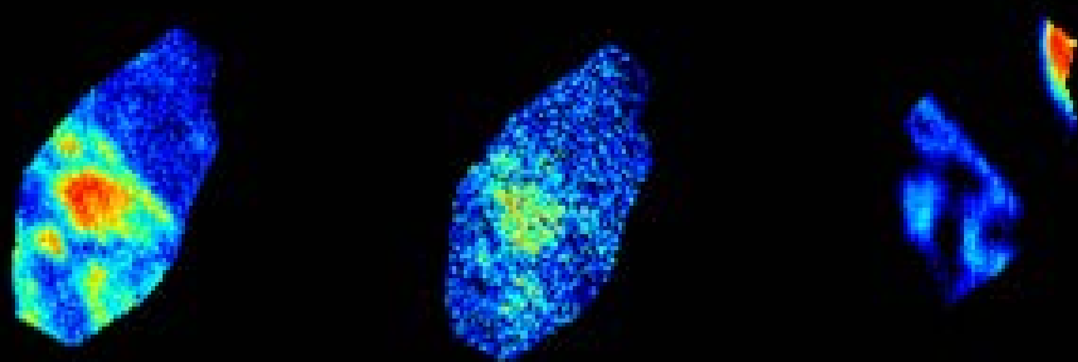

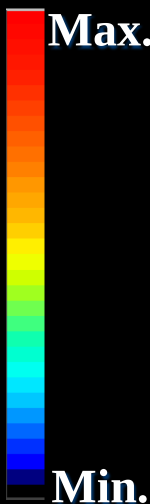


<u>FLOGOPITE</u> (*Mg*, *K* e *F*)

<u>IL Map</u>

# *Conclusions*

• external beams are used in many different fields of applications, such as CH, biology, earth sciences,…

• extraction window and external path are critical parameters to maintain beam quality

• $Si_3N_4$ membranes are the typical, although not the unique, choice for beam exit windows

• a variety of external beam set-ups has been developed so far

• advantages and limitations of these solutions are to  be analyzed in order to find the best solution for the applications of interest

• external micro-beam may constitute the solution to problems where the beam induced damage is critical and high spatial resolution is required, e.g. in many CH studies

# *Thank you for your attention*

*Albrecht Dürer*
*Study of Hands, 1508*
*Brush and ink, highlighted with white on blue tinted paper,*
*29 x 20 cm*
*Graphische Sammlung*
*Albertina, Vienna*

giuntini@fi.infn.it